10-12 October 2012

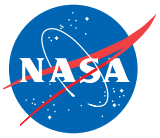

TECH BRIEFS

NATIONAL AERONAUTICS AND SPACE ADMINISTRATION

INTRODUCTION

Tech Briefs are short announcements of innovations originating from research and development activities of the National Aeronautics and Space Administration. They emphasize information considered likely to be transferable across industrial, regional, or disciplinary lines and are issued to encourage commercial application.

Additional Information on NASA Tech Briefs and TSPs

Additional information announced herein may be obtained from the NASA Technical Reports Server: **http://ntrs.nasa.gov**.

Please reference the control numbers appearing at the end of each Tech Brief. Information on NASA's Innovative Partnerships Program (IPP), its documents, and services is available on the World Wide Web at **http://www.ipp.nasa.gov**.

Innovative Partnerships Offices are located at NASA field centers to provide technology-transfer access to industrial users. Inquiries can be made by contacting NASA field centers listed below.

NASA Field Centers and Program Offices

Ames Research Center
David Morse
(650) 604-4724
david.r.morse@nasa.gov

Dryden Flight Research Center
Ron Young
(661) 276-3741
ronald.m.young@nasa.gov

Glenn Research Center
Kimberly A. Dalgleish-Miller
(216) 433-8047
kimberly.a.dalgleish@nasa.gov

Goddard Space Flight Center
Nona Cheeks
(301) 286-5810
nona.k.cheeks@nasa.gov

Jet Propulsion Laboratory
Indrani Graczyk
(818) 354-2241
indrani.graczyk@jpl.nasa.gov

Johnson Space Center
John E. James
(281) 483-3809
john.e.james@nasa.gov

Kennedy Space Center
David R. Makufka
(321) 867-6227
david.r.makufka@nasa.gov

Langley Research Center
Michelle Ferebee
(757) 864-5617
michelle.t.ferebee@nasa.gov

Marshall Space Flight Center
Terry L. Taylor
(256) 544-5916
terry.taylor@nasa.gov

Stennis Space Center
Ramona Travis
(228) 688-3832
ramona.e.travis@ssc.nasa.gov

NASA Headquarters

Daniel Lockney,
Technology Transfer Program Executive
(202) 358-2037
daniel.p.lockney@nasa.gov

Small Business Innovation Research (SBIR) & Small Business Technology Transfer (STTR) Programs
Rich Leshner, Program Executive
(202) 358-4920
rleshner@nasa.gov

TECH BRIEFS

NATIONAL AERONAUTICS AND SPACE ADMINISTRATION

Detection of Chemical Precursors of Explosives

Precursors provide early warning.

Ames Research Center, Moffett Field, California

Certain selected chemicals associated with terrorist activities are too unstable to be prepared in final form. These chemicals are often prepared as precursor components, to be combined at a time immediately preceding the detonation. One example is a liquid explosive, which usually requires an oxidizer, an energy source, and a chemical or physical mechanism to combine the other components. Detection of the oxidizer (e.g. H_2O_2) or the energy source (e.g., nitromethane) is often possible, but must be performed in a short time interval (e.g., 5–15 seconds) and in an environment with a very small concentration (e.g.,1–100 ppm), because the target chemical(s) is carried in a sealed container.

These needs are met by this invention, which provides a system and associated method for detecting one or more chemical precursors (components) of a multi-component explosive compound. Different carbon nanotubes (CNTs) are loaded (by doping, impregnation, coating, or other functionalization process) for detecting of different chemical substances that are the chemical precursors, respectively, if these precursors are present in a gas to which the CNTs are exposed. After exposure to the gas, a measured electrical parameter (e.g. voltage or current that correlate to impedance, conductivity, capacitance, inductance, etc.) changes with time and concentration in a predictable manner if a selected chemical precursor is present, and will approach an asymptotic value promptly after exposure to the precursor.

The measured voltage or current are compared with one or more sequences of their reference values for one or more known target precursor molecules, and a most probable concentration value is estimated for each one, two, or more target molecules. An error value is computed, based on differences of voltage or current for the measured and reference values, using the most probable concentration values. Where the error value is less than a threshold, the system concludes that the target molecule is likely. Presence of one, two, or more target molecules in the gas can be sensed from a single set of measurements.

This work was done by Jing Li of Ames Research Center. Further information is contained in a TSP (see page 1). ARC-15566-5

Detecting Methane From Leaking Pipelines and as Greenhouse Gas in the Atmosphere

Remote detection will speed up response time.

Goddard Space Flight Center, Greenbelt, Maryland

Laser remote sensing measurements of trace gases from orbit can provide unprecedented information about important planetary science and answer critical questions about planetary atmospheres. Methane (CH_4) is the second most important anthropogenically produced greenhouse gas. Though its atmospheric abundance is much less than that of CO_2 (1.78 ppm vs. 380 ppm), it has much larger greenhouse heating potential. CH_4 also contributes to pollution in the lower atmosphere through chemical reactions, leading to ozone production. Atmospheric CH_4 concentrations have been increasing as a result of increased fossil fuel production, rice farming, livestock, and landfills. Natural sources of CH_4 include wetlands, wild fires, and termites, and perhaps other unknown sources. Important sinks for CH_4 include non-saturated soils and oxidation by hydroxyl radicals in the atmosphere.

Remotely measuring CH_4 and other biogenic molecules (such as ethane and formaldehyde) on Mars also has important implications on the existence of life on Mars. Measuring CH_4 at very low (ppb) concentrations from orbit will dramatically improve the sensitivity and spatial resolution in the search for CH_4 vents and sub-surface life on other planets.

A capability has been developed using lasers and spectroscopic detection techniques for the remote measurements of trace gases in open paths. Detection of CH_4, CO_2, H_2O, and CO in absorption cells and in open paths, both in the mid-IR and near-IR region, has been demonstrated using an Optical Parametric Amplifier laser transmitter developed at GSFC. With this transmitter, it would be possible to develop a remote sensing methane instrument.

CH_4 detection also has very important commercial applications. Pipeline leak detection from an aircraft or a helicopter can significantly reduce cost, response time, and pinpoint the location. The main advantage is the ability to rapidly detect CH_4 leaks remotely. This is extremely important for the petrochemical industry. This capability can be used in manned or unmanned airborne platforms for the detection of leaks in pipelines and other areas of interest where a CH_4 leak is suspected.

This work was done by Haris Riris, Kenji Numata, Steve Li, Stewart Wu, Anand Ramanathan, and Martha Dawsey of Goddard Space Flight Center. Further information is contained in a TSP (see page 1). GSC-16184-1

Onboard Sensor Data Qualification in Human-Rated Launch Vehicles

Applications include sensor data qualification and equipment condition monitoring in commercial power plants.

John H. Glenn Research Center, Cleveland, Ohio

The avionics system software for human-rated launch vehicles requires an implementation approach that is robust to failures, especially the failure of sensors used to monitor vehicle conditions that might result in an abort determination. Sensor measurements provide the basis for operational decisions on human-rated launch vehicles. This data is often used to assess the health of system or subsystem components, to identify failures, and to take corrective action. An incorrect conclusion and/or response may result if the sensor itself provides faulty data, or if the data provided by the sensor has been corrupted. Operational decisions based on faulty sensor data have the potential to be catastrophic, resulting in loss of mission or loss of crew. To prevent these later situations from occurring, a Modular Architecture and Generalized Methodology for Sensor Data Qualification in Human-rated Launch Vehicles has been developed.

Sensor Data Qualification (SDQ) is a set of algorithms that can be implemented in onboard flight software, and can be used to qualify data obtained from flight-critical sensors prior to the data being used by other flight software algorithms. Qualified data has been analyzed by SDQ and is determined to be a true representation of the sensed system state; that is, the sensor data is determined not to be corrupted by sensor faults or signal transmission faults. Sensor data can become corrupted by faults at any point in the signal path between the sensor and the flight computer. Qualifying the sensor data has the benefit of ensuring that erroneous data is identified and flagged before otherwise being used for operational decisions, thus increasing confidence in the response of the other flight software processes using the qualified data, and decreasing the probability of false alarms or missed detections.

At a high level, SDQ is called by the flight computer, as required each cycle, to qualify a specific sensor or set of sensors. SDQ first determines the update-rate of the data, and obtains the specified data from the sensor data table. SDQ then consults the data provided by the Mission Manager Function to determine the appropriate subset of pre-defined algorithms, thresholds, and parameters to be used in qualifying specified sensor data. Next, appropriate algorithms are applied to the data. If a given algorithm determines that the data is faulty, the associated data signal accrues a strike from that algorithm for the current flight computer cycle, and the algorithm or algorithms that failed the data are recorded. Having run all applicable fault detection algorithms, the strike counters for each of the applicable algorithm/sensor pairs are then tested for the persistence of any failures. Sensors associated with data that meets persistence criteria are flagged as permanently failed.

Alternate embodiments of some of the qualification algorithms used in the Ares SDQ architecture have prior implementations that were incorporated into commercial data qualification development and analysis tools under the SureSense trademark. SureSense has been used to develop and implement real-time data qualification algorithms for ground-based nuclear power generation systems.

This work was done by Edmond Wong and Kevin J. Melcher of Glenn Research Center; William A. Maul, Amy K. Chicatelli, Thomas S. Sowers, and Christopher Fulton of QinetiQ North America; and Randall Bickford of Expert Microsystems, Inc. Further information is contained in a TSP (see page 1).

Inquiries concerning rights for the commercial use of this invention should be addressed to NASA Glenn Research Center, Innovative Partnerships Office, Attn: Steven Fedor, Mail Stop 4–8, 21000 Brookpark Road, Cleveland, Ohio 44135. Refer to LEW-18633-1.

Rugged, Portable, Real-Time Optical Gaseous Analyzer for Hydrogen Fluoride

Applications include trace gas sensor applications where rapid sampling is required, particularly in human-occupied closed volumes.

John H. Glenn Research Center, Cleveland, Ohio

Hydrogen fluoride (HF) is a primary evolved combustion product of fluorinated and perfluorinated hydrocarbons. HF is produced during combustion by the presence of impurities and hydrogen-containing polymers including polyimides. This effect is especially dangerous in closed occupied volumes like spacecraft and submarines. In these systems, combinations of perfluorinated hydrocarbons and polyimides are used for insulating wiring. HF is both highly toxic and short-lived in closed environments due to its reactivity. The high reactivity also makes HF sampling problematic.

An infrared optical sensor can detect promptly evolving HF with minimal sampling requirements, while providing both high sensitivity and high specificity. A rugged optical path length enhancement architecture enables both high HF sensitivity and rapid environmental sampling with minimal gaseous contact with the low-reactivity sensor surfaces. The inert optical sample cell, combined with infrared semiconductor lasers, is joined with an analog and digital electronic

control architecture that allows for ruggedness and compactness. The combination provides both portability and battery operation on a simple camcorder battery for up to eight hours.

Optical detection of gaseous HF is confounded by the need for rapid sampling with minimal contact between the sensor and the environmental sample. A sensor is required that must simultaneously provide the required sub-parts-per-million detection limits, but with the high specificity and selectivity expected of optical absorption techniques. It should also be rugged and compact for compatibility with operation onboard spacecraft and submarines.

A new optical cell has been developed for which environmental sampling is accomplished by simply traversing the few-mm-thick cell walls into an open volume where the measurement is made. A small, low-power fan or vacuum pump may be used to push or pull the gaseous sample into the sample volume for a response time of a few seconds. The optical cell simultaneously provides for an enhanced optical interaction path length between the environmental sample and the infrared laser. Further, the optical cell itself is comprised of inert materials that render it immune to attack by HF. In some cases, the sensor may be configured so that the optoelectronic devices themselves are protected and isolated from HF by the optical cell. The optical sample cell is combined with custom-developed analog and digital control electronics that provide rugged, compact operation on a platform that can run on a camcorder battery.

The sensor is inert with respect to acidic gases like HF, while providing the required sensitivity, selectivity, and response time. Certain types of combustion events evolve copious amounts of HF, very little of other gases typically associated with combustion (e.g., carbon monoxide), and very low levels of aerosols and particulates (which confound traditional smoke detectors). The new sensor platform could warn occupants early enough to take the necessary countermeasures.

This work was done by Jeffrey Pilgrim and Paula Gonzales of Vista Photonics, Inc. for Glenn Research Center. Further information is contained in a TSP (see page 1).

Inquiries concerning rights for the commercial use of this invention should be addressed to NASA Glenn Research Center, Innovative Partnerships Office, Attn: Steven Fedor, Mail Stop 4–8, 21000 Brookpark Road, Cleveland, Ohio 44135. Refer to LEW-18892-1.

A Probabilistic Mass Estimation Algorithm for a Novel 7-Channel Capacitive Sample Verification Sensor

NASA's Jet Propulsion Laboratory, Pasadena, California

A document describes an algorithm created to estimate the mass placed on a sample verification sensor (SVS) designed for lunar or planetary robotic sample return missions. A novel SVS measures the capacitance between a rigid bottom plate and an elastic top membrane in seven locations. As additional sample material (soil and/or small rocks) is placed on the top membrane, the deformation of the membrane increases the capacitance. The mass estimation algorithm addresses both the calibration of each SVS channel, and also addresses how to combine the capacitances read from each of the seven channels into a single mass estimate. The probabilistic approach combines the channels according to the variance observed during the training phase, and provides not only the mass estimate, but also a value for the certainty of the estimate.

SVS capacitance data is collected for known masses under a wide variety of possible loading scenarios, though in all cases, the distribution of sample within the canister is expected to be approximately uniform. A capacitance-vs-mass curve is fitted to this data, and is subsequently used to determine the mass estimate for the single channel's capacitance reading during the measurement phase. This results in seven different mass estimates, one for each SVS channel. Moreover, the variance of the calibration data is used to place a Gaussian probability distribution function (pdf) around this mass estimate. To blend these seven estimates, the seven pdfs are combined into a single Gaussian distribution function, providing the final mean and variance of the estimate. This blending technique essentially takes the final estimate as an average of the estimates of the seven channels, weighted by the inverse of the channel's variance.

This work was done by Michael Wolf of Caltech for NASA's Jet Propulsion Laboratory. Further information is contained in a TSP (see page 1). NPO-48143

Low-Power Architecture for an Optical Life Gas Analyzer

A simple camcorder battery can be used for as long as eight hours.

John H. Glenn Research Center, Cleveland, Ohio

Analog and digital electronic control architecture has been combined with an operating methodology for an optical trace gas sensor platform that allows very low power consumption while providing four independent gas measurements in essentially real time, as well as a user interface and digital data storage and output. The implemented design eliminates the cross-talk between the measurement channels while maximizing the sensitivity, selectivity, and dynamic range for each measured gas. The combination provides for battery operation on a simple camcorder battery for as long as eight hours. The custom, compact, rugged, self-contained design specifically targets applications of optical major constituent and trace gas detection for multiple gases using multiple lasers and photodetectors in an integrated package.

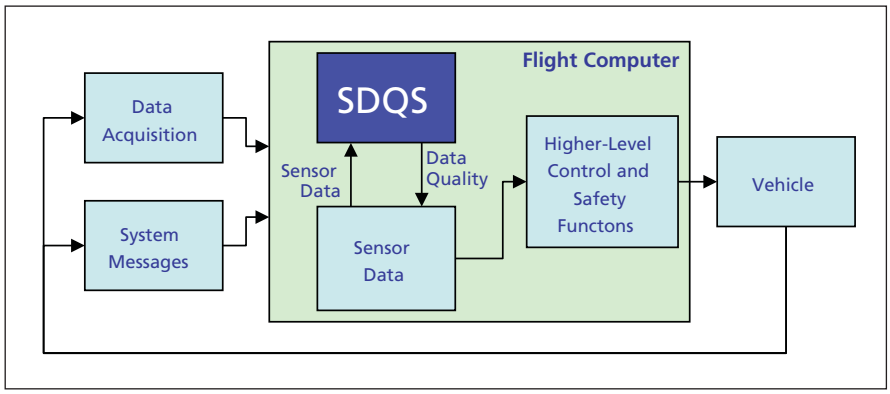

The **Sensor Data Qualification** (SDQ) system receives inputs from system messages and data acquisition. The sensor data includes first-stage and upper-stage flight-critical sensors.

Commercial off-the-shelf digital electronics including data acquisition cards (DAQs), complex programmable logic devices (CPLDs), field programmable gate arrays (FPGAs), and microcontrollers have been used to achieve the desired outcome. The lowest-power integrated architecture achieved during the project was realized in the prototype that utilized a custom FPGA digital board (in combination with a custom-built, low-power analog electronics board) and a low-performance commercial microcontroller. The FPGA generated all the necessary control signals for the analog board, and performed data acquisition and low-level, time-critical data processing. The microcontroller was used to implement high-level data analysis, the user interface, and data storage and output. Further power savings were realized by operating the four lasers sequentially, rather than operating them in parallel. A several-Hz update rate was achieved even with sequential operation, much faster than required for gas measurement on the International Space Station.

A rugged and flexible multiple gas sensor platform was developed, which involves laser diode-based optical absorption spectroscopy coupled to an elegant optical path length enhancement solution and advanced digital and analog electronic design. The optical absorption cell is shared by multiple lasers and detectors, which minimizes the footprint of the device. On the other hand, the optical layout is simple and flexible: no precise alignment is required. The laser diodes are easily interchangeable, which, in principle, allows reconfiguring the sensor to measure different sets of trace gases. Custom power-efficient analog and digital electronic boards are designed to minimize the power consumption of the sensor. Further power savings are realized by fast time-multiplexing the measurements of different gases, rather than implementing them in parallel. This development allows a fully integrated multiple gas monitor to operate on simple camcorder batteries for a period of several hours.

This work was done by Jeffrey Pilgrim and Andrei Vakhtin of Vista Photonics, Inc. for Glenn Research Center. Further information is contained in a TSP (see page 1).

Inquiries concerning rights for the commercial use of this invention should be addressed to NASA Glenn Research Center, Innovative Partnerships Office, Attn: Steven Fedor, Mail Stop 4–8, 21000 Brookpark Road, Cleveland, Ohio 44135. Refer to LEW-18894-1.

Online Cable Tester and Rerouter

This technology enables proactive detection of impending cable failures, allowing for function rerouting.

John F. Kennedy Space Center, Florida

Hardware and algorithms have been developed to transfer electrical power and data connectivity safely, efficiently, and automatically from an identified damaged/defective wire in a cable to an alternate wire path. The combination of online cable testing capabilities, along with intelligent signal rerouting algorithms, allows the user to overcome the inherent difficulty of maintaining system integrity and configuration control, while autonomously rerouting signals and functions without introducing new failure modes. The incorporation of this capability will increase the reliability of systems by ensuring system availability during operations.

The operation of the innovation is based on the injection of a low-level and short-duration signal into a wire under test. The cable router master unit consists of a pulse generator, a multiplexer, a switch matrix, and a detector circuit. The pulse generator provides a step pulse that is applied to the multiplexer. The multiplexer, in turn, routes the test pulse to one of many wires. The signal then propagates through the selected wire until it reaches the cable route slave circuit. The slave circuit monitors the wire, and once it receives the signal, it routes it back to the master unit through a communication wire. The detector circuit in the master unit then determines the presence of the signal to indicate that a good connection is in place. The absence of the test pulse becomes an indication of a faulty connection. A plurality of communication wires is used, so that the individual state of health is not a determining factor for the analysis of the health of the wire(s) under test.

The master unit sequentially scans all the wires selected as "active" or "spares." The current implementation of the online rerouter system can monitor up to eight wires. However, the circuit can be expanded to monitor a larger number of wires. The wires can be independently assigned to be "active" or to be "spares." Once an active wire has been labeled as failed, the master and the slave units communicate with each other, and immediately route the signals that were flowing through the failed wire to one of the spare wires. This allows for the system to maintain integrity with a disruption shorter than one second in the current implementation.

The small amplitude of the test pulse injected into the wires requires multiple successive measurements to assess the integrity of the wire. The test pulse level has to be maintained at a low level in order not to interfere with signals being carried in the wire under test. This allows for discrimination between a large, non-correlated signal and a small, synchronous test pulse without interfering with the operation of the wire.

This work was done by Mark Lewis of Kennedy Space Center and Pedro Medelius of ASRC Aerospace Corporation. For more information, contact the Kennedy Space Center Innovative Partnerships Office at 321-867-5033. KSC-13440

A Three-Frequency Feed for Millimeter-Wave Radiometry

This wave feed operates at frequencies approximately five times higher than current feeds and provides greater bandwidth.

NASA's Jet Propulsion Laboratory, Pasadena, California

A three-frequency millimeter-wave feed horn was developed as part of an advanced component technology task that provides components necessary for higher-frequency radiometers to meet the needs of the Surface Water and Ocean Topography (SWOT) mission. The primary objectives of SWOT are to characterize ocean sub-mesoscale processes on 10-km and larger scales in the global oceans, and to measure the global water storage in inland surface water bodies, including rivers, lakes, reservoirs, and wetlands.

In this innovation, the feed provides three separate output ports in the 87-to-97-GHz, 125-to-135-GHz, and 161-to-183-GHz bands; WR10 for the 90-GHz channel, WR8 for the 130-GHz channel, and WR5 for the 170-GHz channel. These ports are in turn connected to individual radiometer channels that will also demonstrate component technology including new PIN-diode switches and noise diodes for internal calibration integrated into each radiometer front end. For this application, a prime focus feed is required with an edge taper of approximately 20 dB at an illumination angle of ±40°. A single polarization is provided in each band. Preliminary requirements called for a return loss of better than 15 dB, which is achieved across all three bands. Good pattern symmetry is also obtained throughout all three-frequency bands. This three-frequency broadband millimeter-wave feed also minimizes mass and provides a common focal point for all three millimeter-wave bands.

In order to achieve similar E and H plane beam widths over the combined 87-to-183-GHz band ring, loaded slots are employed in the corrugated portion of the feed. The feed operates in a flare-angle limited condition, which gives approximately constant beam width across the entire band, and provides a common phase center located near its apex.

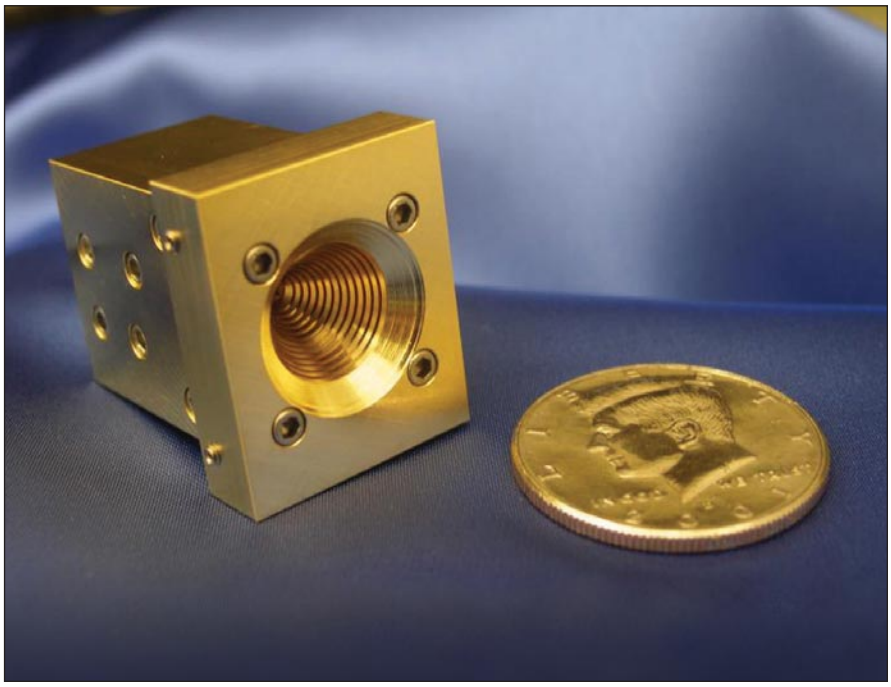

The assembled prototype **Three-Frequency Feed** is shown, with the low-frequency combiner absent, along with a half-dollar coin for scale. The overall size of the feed, including the combiner block, is approximately 1×1.25×1.5 in. (≈2.5×3.2×3.8 cm).

The half-flare angle for the feed is approximately 30°. Analysis and optimization of the overall feed design employed a combination of finite element and mode-matching tools.

The illumination requirements and relative frequency spacing for this application are similar to those required for the Scanning Multichannel Microwave Radiometer (SMMR) on Seasat, the (TOPEX)/Poseidon, and the Jason missions. However, in this particular application the required fractional bandwidth is larger. Thus, while the three-frequency feed horn described here shares many features in common with the feed previously developed for the above missions, enhancements are necessary in order to achieve broad band performance and manufacturability in the millimeter-wave bands.

This work was done by Daniel J. Hoppe, Behrouz Khayatian, John B. Sosnowski, Alan K. Johnson, and Peter J. Bruneau of Caltech for NASA's Jet Propulsion Laboratory. For more information, contact iaoffice@jpl.nasa.gov. NPO-48528

Capacitance Probe Resonator for Multichannel Electrometer

NASA's Jet Propulsion Laboratory, Pasadena, California

A multichannel electrometer voltmeter has been developed that employs a mechanical resonator with voltage-sensing capacitance-probe electrodes that enable high-impedance, high-voltage, radiation-hardened measurement of an Internal Electrostatic Discharge Monitor (IESDM) sensor. The IESDM is new sensor technology targeted for integration into a Space Environmental Monitor (SEM) subsystem used for the characterization and monitoring of deep dielectric charging on spacecraft.

The resonator solution relies on a non-contact, voltage-sensing, sinusoidal-varying capacitor to achieve input impedances as high as 10 petaohms as determined by the resonator materials, geometries, cleanliness, and construction. The resonator is designed with one dominant mechanical degree of freedom, so it resonates as a simple harmonic oscillator and because of the linearity of the variable sense capacitor to displacement, generates a pure sinusoidal current signal for a fixed input voltage under measurement. This enables the use of an idealized phase-lock sensing scheme for optimal signal detection in the presence of noise.

This work was done by Brent R. Blaes, Rembrandt T. Schaefer, and Robert J. Glaser of Caltech for NASA's Jet Propulsion Laboratory. Further information is contained in a TSP (see page 1). NPO-47335

Inverted Three-Junction Tandem Thermophotovoltaic Modules

John H. Glenn Research Center, Cleveland, Ohio

An InGaAs-based three-junction (3J) tandem thermophotovoltaic (TPV) cell has been investigated to utilize more of the blackbody spectrum (from a 1,100 °C general purpose heat source — GPHS) efficiently. The tandem consists of three vertically stacked subcells, a 0.74-eV InGaAs cell, a 0.6-eV InGaAs cell, and a 0.55-eV InGaAs cell, as well as two interconnecting tunnel junctions.

A >20% TPV system efficiency was achieved by another group with a 1,040 °C blackbody using a single-bandgap 0.6-eV InGaAs cell MIM (monolithic interconnected module) (30 lateral junctions) that delivered about 12 V/30 or 0.4 V/junction. It is expected that a three-bandgap tandem MIM will eventually have about 3× this voltage (1.15 V) and about half the current. A 4 A/cm^2 would be generated by a single-bandgap 0.6-V InGaAs MIM, as opposed to the 2 A/cm^2 available from the same spectrum when split among the three series-connected junctions in the tandem stack. This would then be about a 50%

increase ($3\times V_{oc}$, $0.5\times I_{sc}$) in output power if the proposed tandem replaced the single-bandgap MIM.

The advantage of the innovation, if successful, would be a 50% increase in power conversion efficiency from radioisotope heat sources using existing thermophotovoltaics. Up to 50% more power would be generated for radioisotope GPHS deep space missions. This type of InGaAs multijunction stack could be used with terrestrial concentrator solar cells to increase efficiency from 41 to 45% or more.

This work was done by Steven Wojtczuk of Spire Semiconductor for Glenn Research Center. Further information is contained in a TSP (see page 1).

Inquiries concerning rights for the commercial use of this invention should be addressed to NASA Glenn Research Center, Innovative Partnerships Office, Attn: Steven Fedor, Mail Stop 4–8, 21000 Brookpark Road, Cleveland, Ohio 44135. Refer to LEW-18909-1.

Fabrication of Single Crystal MgO Capsules

Lyndon B. Johnson Space Center, Houston, Texas

A method has been developed for machining MgO crystal blocks into forms for containing metallic and silicate liquids at temperatures up to 2,400 °C, and pressures up to at least 320 kilobars. Possible custom shapes include tubes, rods, insulators, capsules, and guides. Key differences in this innovative method include drilling along the crystallographic zone axes, use of a vibration minimizing material to secure the workpiece, and constant flushing of material swarf with a cooling medium/lubricant (water).

A single crystal MgO block is cut into a section ≈5 mm thick, 1 cm on a side, using a low-speed saw with a 0.004 blade. The cut is made parallel to the direction of cleavage. The block may be cut to any thickness to achieve the desired length of the piece. To minimize drilling vibrations, the MgO block is mounted on a piece of adhesive putty in a vise. The putty wad cradles the bottom half of the entire block. Diamond coring tools are used to drill the MgO to the desired custom shape, with water used to wet and wash the surface of swarf. Compressed air may also be used to remove swarf during breaks in drilling. The MgO workpiece must be kept cool at all times with water. After all the swarf is rinsed off, the piece is left to dry overnight.

If the workpiece is still attached to the base of the MgO block after drilling, it may be cut off by using a diamond cutoff wheel on a rotary hand tool or by using a low-speed saw.

This work was done by Lisa Danielson of Jacobs Technology for Johnson Space Center. Further information is contained in a TSP (see page 1). ***MSC-25052-1***

Inflatable Hangar for Assembly of Large Structures in Space

Such hangars may greatly increase the dexterity and performance of astronauts by operating in a shirtsleeves environment during the assembly process.

NASA's Jet Propulsion Laboratory, Pasadena, California

The NASA Human Space Flight program is interested in projects where humans, beyond low-Earth orbit (LEO), can make an important and unique contribution that cannot be reasonably accomplished purely by robotic means, and is commensurate with the effort and cost associated with human spaceflight.

Robotic space telescope missions have been conceived and launched as completed assemblies (e.g., Hubble) or as "jack-in-the-box" one-time deployments (e.g., James Webb). If it were possible to assemble components of a very large telescope from one or two launches into a telescope that was vastly greater in light-gathering power and resolution, that would constitute a breakthrough. Large telescopes on Earth, like all one-off precision assembly tasks, are done by humans. Humans in shirtsleeves (or cleanroom "bunny suits") can perform tasks of remarkable dexterity and precision. Unfortunately, astronauts in pressure suits cannot perform such dexterous and precise tasks because of the limitations of the pressurized gloves.

If a large, inflatable "hangar" were placed in high orbit, along with all the

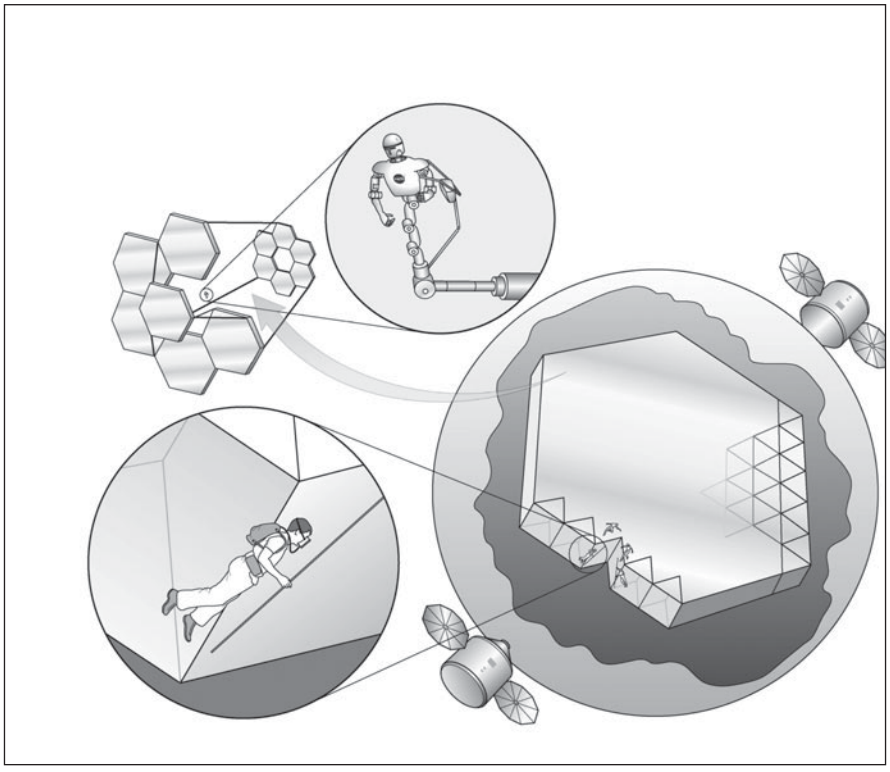

An artist's rendering of the **Shirtsleeves Assembly Hangar**. At the lower right is a cutaway of the inflated fabric sphere that houses astronauts in oxygen masks and backpacks. The humans would work with a robot to accomplish the final telescope assembly.

components needed for a large assembly such as a large telescope, then humans in bunny suits could perform the same sorts of extremely precise and dexterous assembly that they could be expected to perform on Earth. Calculations show that such an inflatable hangar, and the necessary gas to make it safe to occupy by shirtsleeves humans wearing oxygen masks, fits within the mass and volume limitations of the proposed "Space Launch System" heavy-lift rocket. A second launch could bring up all the components of a ≈100-meter-diameter or larger telescope.

A large [200 ft (≈61 m) in diameter] inflated fabric sphere (or hangar) would contain four humans in bunny suits. The sphere would contain sufficient atmospheric pressure so that spacesuits would not be necessary [about 3.2 psi (≈22 kPa)]. The humans would require only oxygen masks and small backpacks similar to SCUBA tanks. The oxygen content of the gas would be about 35%, low enough to reduce fire risk but high enough to sustain life in the event of a failure of an oxygen mask. The bunny-suited astronauts could ride on long "cherry-picker" robots with foot restraints somewhat similar to the arm on the International Space Station. Other astronauts would maneuver freely with small propeller fans on their backpacks to provide thrust in the zero-g environment.

This work was done by Brian H. Wilcox of Caltech for NASA's Jet Propulsion Laboratory. Further information is contained in a TSP (see page 1). ***NPO-48441***

Mars Aqueous Processing System

This technology can be used in treating soil contaminated with heavy metals and remediation of acid mine drainage.

Lyndon B. Johnson Space Center, Houston, Texas

The goal of the Mars Aqueous Processing System (MAPS) is to establish a flexible process that generates multiple products that are useful for human habitation. Selectively extracting useful components into an aqueous solution, and then sequentially recovering individual constituents, can obtain a suite of refined or semi-refined products. Similarities in the bulk composition (although not necessarily of the mineralogy) of Martian and Lunar soils potentially make MAPS widely applicable. Similar process steps can be conducted on both Mars and Lunar soils while tailoring the reaction extents and recoveries to the specifics of each location.

The MAPS closed-loop process selectively extracts, and then recovers, constituents from soils using acids and bases. The emphasis on Mars involves the production of useful materials such as iron, silica, alumina, magnesia, and concrete with recovery of oxygen as a byproduct. On the Moon, similar chemistry is applied with emphasis on oxygen production.

This innovation has been demonstrated to produce high-grade materials, such as metallic iron, aluminum oxide, magnesium oxide, and calcium oxide, from lunar and Martian soil simulants. Most of the target products exhibited purities of 80 to 90 percent or more, allowing direct use for many potential applications. Up to one-fourth of the feed soil mass was converted to metal, metal oxide, and oxygen products. The soil residue contained elevated silica content, allowing for potential additional refining and extraction for recovery of materials needed for photovoltaic, semiconductor, and glass applications.

A high-grade iron oxide concentrate derived from lunar soil simulant was used to produce a metallic iron component using a novel, combined hydrogen reduction/metal sintering technique. The part was subsequently machined and found to be structurally sound. The behavior of the lunar-simulant-derived iron product was very similar to that produced using the same methods on a Michigan iron ore concentrate, which demonstrates that lunar-derived material can be used in a manner similar to conventional terrestrial iron. Metallic iron was also produced from the Mars soil simulant.

The aluminum and magnesium oxide products produced by MAPS from lunar and Mars soil simulants exhibited excellent thermal stability, and were shown to be capable of use for refractory oxide structural materials, or insulation at temperatures far in excess of what could be achieved using unrefined soils. These materials exhibited the refractory characteristics needed to support iron casting and forming operations, as well as other thermal processing needs.

Extraction residue samples contained up to 79 percent silica. Such samples were successfully fused into a glass that exhibited high light transmittance.

This work was done by Mark Berggren, Cherie Wilson, Stacy Carrera, Heather Rose, Anthony Muscatello, James Kilgore, and Robert Zubrin of Pioneer Astronautics for Johnson Space Center. Further information is contained in a TSP (see page 1). ***MSC-23885-1/4362-1***

Hybrid Filter Membrane

Uses for this device include battle tanks, remote command centers, field hospitals, and nuclear power plants.

John H. Glenn Research Center, Cleveland, Ohio

Cabin environmental control is an important issue for a successful Moon mission. Due to the unique environment of the Moon, lunar dust control is one of the main problems that significantly diminishes the air quality inside spacecraft cabins. Therefore, this innovation was motivated by NASA's need to minimize the negative health impact that air-suspended lunar dust particles have on astronauts in spacecraft cabins.

It is based on fabrication of a hybrid filter comprising nanofiber nonwoven layers coated on porous polymer membranes with uniform cylindrical pores. This design results in a high-efficiency gas particulate filter with low pressure drop and the ability to be easily regenerated to restore filtration performance.

A hybrid filter was developed consisting of a porous membrane with uniform, micron-sized, cylindrical pore channels coated with a thin nanofiber layer. Compared to conventional filter media such as a high-efficiency particulate air (HEPA) filter, this filter is designed to provide high particle efficiency, low pressure drop, and the ability to be regenerated. These membranes have well-defined micron-sized pores and can be used independently as air filters with discreet particle size cut-off, or coated with nanofiber layers for filtration of ultrafine nanoscale particles. The filter consists of a thin design intended to facilitate filter regeneration by localized air pulsing.

The two main features of this invention are the concept of combining a micro-engineered straight-pore membrane with nanofibers. The micro-engineered straight pore membrane can be prepared with extremely high precision. Because the resulting membrane pores are straight and not tortuous like those found in conventional filters, the pressure drop across the filter is significantly reduced. The nanofiber layer is applied as a very thin coating to enhance filtration efficiency for fine nanoscale particles. Additionally, the thin nanofiber coating is designed to promote capture of dust particles on the filter surface and to facilitate dust removal with pulse or back airflow.

This work was done by Castro Laicer, Brian Rasimick, and Zachary Green of Giner Electrochemical Systems, LLC for Glenn Research Center. Further information is contained in a TSP (see page 1).

Inquiries concerning rights for the commercial use of this invention should be addressed to NASA Glenn Research Center, Innovative Partnerships Office, Attn: Steven Fedor, Mail Stop 4–8, 21000 Brookpark Road, Cleveland, Ohio 44135. Refer to LEW-18922-1.

Design for the Structure and the Mechanics of Moballs

Moballs could be used to explore Mars and other windy bodies of the solar system such as Titan.

NASA's Jet Propulsion Laboratory, Pasadena, California

The moball is envisioned to be a round, self-powered, and wind-driven multifunctioning sensor used in the Gone with the Wind ON-Mars (GOWON) [http://www.lpi.usra.edu/meetings/marsconcepts2012/pdf/4238.pdf]: A Wind-Driven Networked System of Mobile sensors on Mars. The moballs would have sensing, processing, and communication capabilities. The moballs would perform in situ detection of key environmental elements such as vaporized water, trace gases, wind, dust, clouds, light and UV exposure, temperature, as well as minerals of interest, possible biosignatures, surface magnetic and electric fields, etc. The embedded various low-power micro instruments could include a Multispectral Microscopic Imager (to detect various minerals), a compact curved focal plane array camera (UV/Vis/NIR) with a large field of view, a compact UV/Visible spectrometer, a micro-weather station, etc. The moballs could communicate with each other and an orbiter. Their wind- or gravity-driven rolling movement could be used to harvest and store electric energy. They could also generate and store energy using the sunlight, when available, and the diurnal temperature variations on Mars. The moballs would be self-aware of their (and their neighbors') positions, energy storage, and memory availability; they would have processing power and could intelligently cooperate with neighboring moballs by distributing tasks, sharing data, and fusing information. The major advantages of using the wind-driven and spherical moball network over rovers or other fixed sensor webs to explore Mars would be: (1) moballs could explore a much larger expanse of Mars in a much faster fashion, (2) they could explore the difficult terrains such as steep slopes and sand dunes, and (3) they would be self-energy-generating and could work together and move around autonomously.

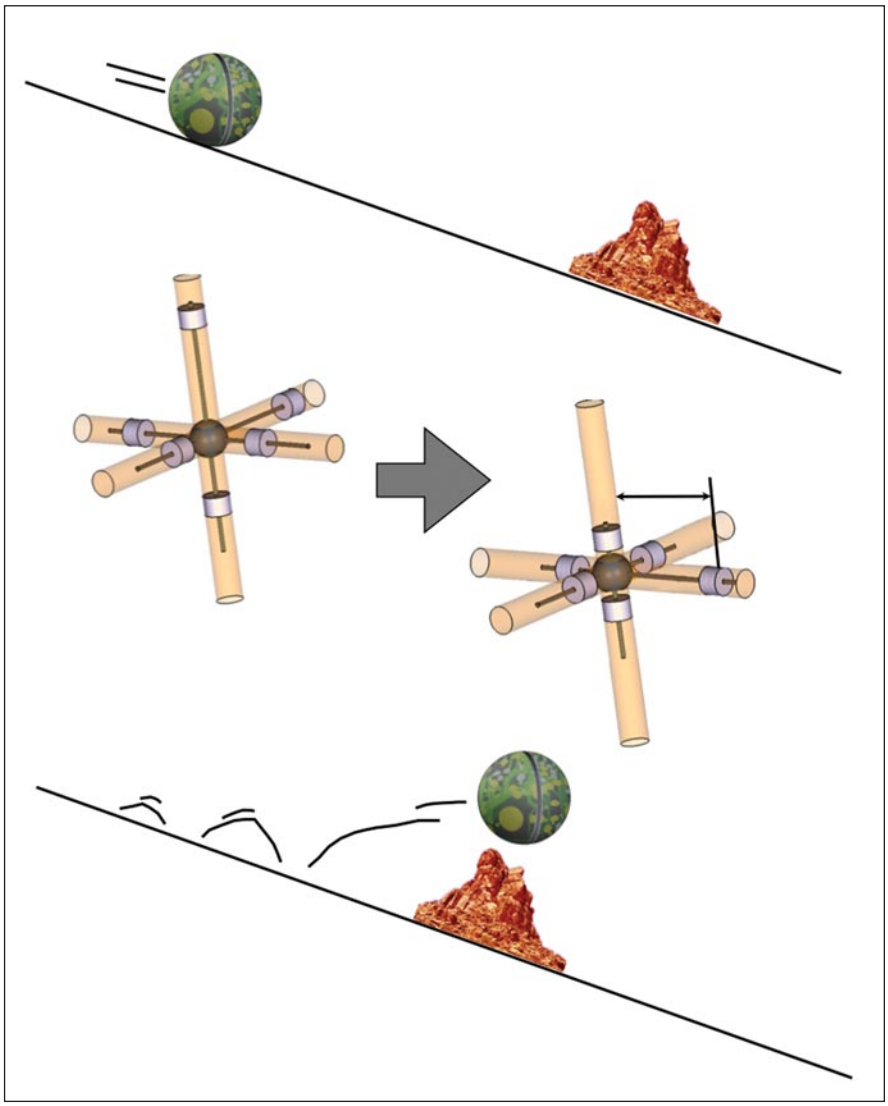

Moballs are able to recognize sharp objects as well as their speed and direction. Based on algorithms already provided in the controller, they can decide when and how to change weights in order to avoid obstacles or jump over them.

The challenge in designing the structure and the mechanics of the moball would be that it should be sturdy enough to withstand the impact of its initial fall, as well as other impacts from obstacles in its way. A mechanism would be needed that could enable hundreds of moballs to be carried while they would be deflated and compact, then would inflate them just after deploying them to their drop site. Furthermore, the moballs should also be light enough to allow them to move easily over obstacles by force of the wind. They also should have some kind of maneuvering mechanism in place to help them avoid very hazardous sharp objects or events, and to enable them to get closer to the objects of interest.

The structure of the moballs was designed so that they would have different layers. The outer layer should comprise a sturdy, yet light, polymer that could

withstand both the impact of the initial drop, as well as the impact of the different obstacles it would encounter while traversing the surface of Mars. This polymer should not deteriorate with the 100 K daily temperature swings on Mars. The inner layer should consist of a very light gas such as nitrogen or helium. In terms of maneuvering, six very light weights placed at strategic locations would give moballs the ability to turn, or even hop, over hazardous (e.g., sharp) obstacles, or even initiate a movement (before getting more help from the wind to be carried around) when stuck. Maneuvering would be necessary in order to get closer to objects of interest. If the weights would be allowed to move freely, they could also be used to generate energy.

To deploy the moballs, NASA Standard Initiators (NSIs) would carry a light gas in the middle, and a few NSIs in the outer layer would carry the liquid form of a selected polymer. As soon as the moballs would get released by the deployer, the inner capsule would be exploded and the gas would fill out the inner layer of the moball, making it round. The NSI capsules containing the special polymer would then be broken, releasing the polymer that fills out the outer layer. In this manner, hundreds or even thousands of deflated moballs could be compacted inside the deployer and inflated just after the deployment and before their initial drop.

For the inner sphere of the moball, three principal (*XYZ*) axes with movable weights inside them would be constructed. The movable weights could be used to balance the motion of the moball. In this manner, the trajectory of the sphere could be corrected with a motorized controller that sits in the center of the sphere and that would control the distance of each weight from the center. This system of weights could be used to deflect the trajectory of the moball. If the weights would be magnet, they could generate power while tumbling around too.

The design described here (in terms of the inner and outer layer, and the three principal axes with controllable weights) would be novel. No pump would be required to deflate or inflate the moballs, saving power, and also reducing the risk of failure. However, it is emphasized that the novelty in this design would make the "hopping" movement of the moball much easier than earlier methods. Previous techniques for making a spherically-shaped robot hop over an object on Mars have assumed that the initial condition of the robot was stationary, i.e., the robot would hop from a position of complete stillness. This would be difficult to do on Mars, since the gravity is around 1/3 of the gravity of Earth, making the reaction force much less than what one would expect. However, since the moballs proposed here would be in a wind-driven (or downward rolling) movement already, they would have an "initial velocity," which would make hopping all the more easy. This is believed to be the most possible way of hopping over a hazardous object on Mars.

This work was done by Faranak Davoodi of Caltech and Farhooman Davoudi, Technical Consultant, for NASA's Jet Propulsion Laboratory.. For more information, contact iaoffice@jpl.nasa.gov.

In accordance with Public Law 96-517, the contractor has elected to retain title to this invention. Inquiries concerning rights for its commercial use should be addressed to:

Innovative Technology Assets Management
JPL
Mail Stop 202-233
4800 Oak Grove Drive
Pasadena, CA 91109-8099
E-mail: iaoffice@jpl.nasa.gov

Refer to NPO-48643, volume and number of this NASA Tech Briefs *issue, and the page number.*

Pressure Dome for High-Pressure Electrolyzer

External gas pressure permits higher pressure and more versatile electrolyzer.

John H. Glenn Research Center, Cleveland, Ohio

A high-strength, low-weight pressure vessel dome was designed specifically to house a high-pressure [2,000 psi (≈13.8 MPa)] electrolyzer. In operation, the dome is filled with an inert gas pressurized to roughly 100 psi (≈690 kPa) above the high, balanced pressure product oxygen and hydrogen gas streams. The inert gas acts to reduce the clamping load on electrolyzer stack tie bolts since the dome pressure acting axially inward helps offset the outward axial forces from the stack gas pressure. Likewise, radial and circumferential stresses on electrolyzer frames are minimized. Because the dome is operated at a higher pressure than the electrolyzer product gas, any external electrolyzer leak prevents oxygen or hydrogen from

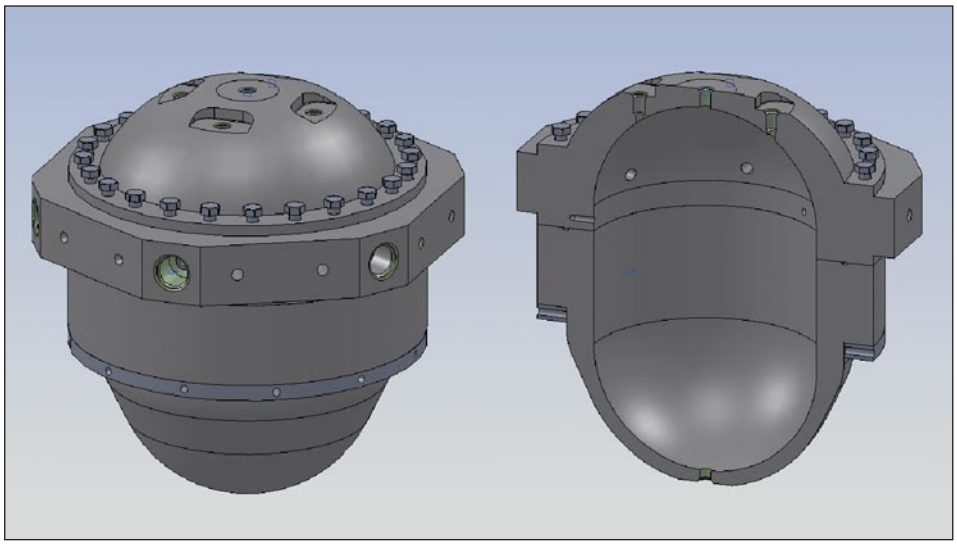

The **Pressure Dome** consists of two machined segments. An O-ring is placed in a groove in the flange of the bottom segment and is trapped by the flange on the top dome segment when these components are bolted together with high-strength bolts.

leaking into the dome. Instead the affected stack gas stream pressure rises detectably, thereby enabling a system shutdown. All electrical and fluid connections to the stack are made inside the pressure dome and require special plumbing and electrical dome interfaces for this to be accomplished. Further benefits of the dome are that it can act as a containment shield in the unlikely event of a catastrophic failure.

Studies indicate that, for a given active area (and hence, cell ID), frame outside diameter must become ever larger to support stresses at higher operating pressures. This can lead to a large footprint and increased costs associated with thicker and/or larger diameter endplates, tie-rods, and the frames themselves. One solution is to employ rings that fit snugly around the frame. This complicates stack assembly and is sometimes difficult to achieve in practice, as its success is strongly dependent on frame and ring tolerances, gas pressure, and operating temperature. A pressure dome permits an otherwise low-pressure stack to operate at higher pressures without growing the electrolyzer hardware.

The pressure dome consists of two machined segments. An O-ring is placed in an O-ring groove in the flange of the bottom segment and is trapped by the flange on the top dome segment when these components are bolted together with high-strength bolts. The pressure dome has several unique features. It is made (to ASME Pressure Vessel guidelines) in a high-strength aluminum alloy with the strength of stainless steel and the weight benefits of aluminum. The flange of the upper dome portion contains specially machined flats for mounting the dome, and other flats dedicated to the special feedthroughs for electrical connections. A pressure dome can be increased in length to house larger stacks (more cells) of the same diameter with the simple addition of a cylindrical segment.

To aid in dome assembly, two stainless steel rings are employed. One is used beneath the heads of the high-strength bolts in lieu of individual hardened washers, and another is used instead of individual nuts. Like electrolyzers could be operated at low or high pressures simply by operating the electrolyzer outside or inside a pressurized dome.

This work was done by Timothy Norman and Edwin Schmitt of Giner Electrochemical Systems, LLC for Glenn Research Center. Further information is contained in a TSP (see page 1).

Inquiries concerning rights for the commercial use of this invention should be addressed to NASA Glenn Research Center, Innovative Partnerships Office, Attn: Steven Fedor, Mail Stop 4–8, 21000 Brookpark Road, Cleveland, Ohio 44135. Refer to LEW-18772-1.

Cascading Tesla Oscillating Flow Diode for Stirling Engine Gas Bearings

John H. Glenn Research Center, Cleveland, Ohio

Replacing the mechanical check-valve in a Stirling engine with a micromachined, non-moving-part flow diode eliminates moving parts and reduces the risk of microparticle clogging.

At very small scales, helium gas has sufficient mass momentum that it can act as a flow controller in a similar way as a transistor can redirect electrical signals with a smaller bias signal. The innovation here forces helium gas to flow in predominantly one direction by offering a clear, straight-path microchannel in one direction of flow, but then through a sophisticated geometry, the reversed flow is forced through a tortuous path. This redirection is achieved by using microfluid channel flow to force the much larger main flow into this tortuous path.

While microdiodes have been developed in the past, this innovation cascades Tesla diodes to create a much higher pressure in the gas bearing supply plenum. In addition, the special shape of the leaves captures loose particles that would otherwise clog the microchannel of the gas bearing pads.

This work was done by Rodger Dyson for Glenn Research Center. Further information is contained in a TSP (see page 1).

Inquiries concerning rights for the commercial use of this invention should be addressed to NASA Glenn Research Center, Innovative Partnerships Office, Attn: Steven Fedor, Mail Stop 4–8, 21000 Brookpark Road, Cleveland, Ohio 44135. Refer to LEW-18862-1.

Compact, Low-Force, Low-Noise Linear Actuator

This actuator has potential uses in military and automotive applications.

NASA's Jet Propulsion Laboratory, Pasadena, California

Actuators are critical to all the robotic and manipulation mechanisms that are used in current and future NASA missions, and are also needed for many other industrial, aeronautical, and space activities. There are many types of actuators that were designed to operate as linear or rotary motors, but there is still a need for low-force, low-noise linear actuators for specialized applications, and the disclosed mechanism addresses this need.

A simpler implementation of a rotary actuator was developed where the end effector controls the motion of a brush for cleaning a thermal sensor. The mechanism uses a SMA (shape-memory alloy) wire for low force, and low noise. The linear implementation of the actuator incorporates a set of springs and mechanical hard-stops for resetting and fault tolerance to mechanical resistance. The actuator can be designed to work in a pull or push mode, or both. Depending on the volume envelope criteria, the actuator can be configured for scaling its volume down to 4×2×1 cm^3. The actuator design

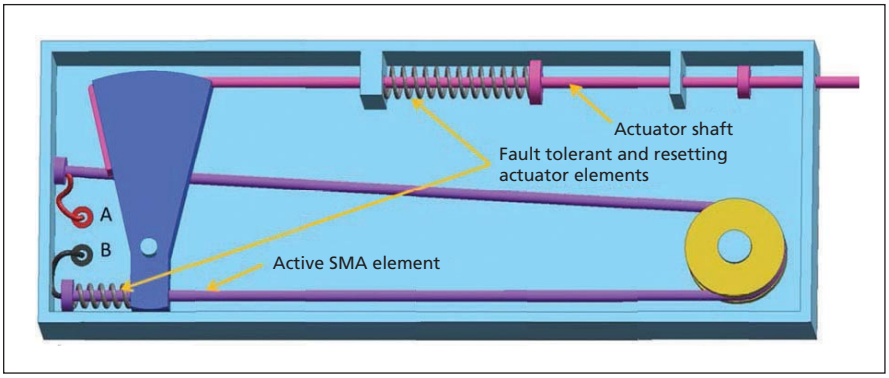

The **Actuator** is driven by shape memory alloy as a primary active element. Electrical connections to points A and B are used to apply electrical power in the resistive NiTi wire, causing a phase change that contracts the wire on the order of 5%.

has an inherent fault tolerance to mechanical resistance. The actuator has the flexibility of being designed for both linear and rotary motion. A specific configuration was designed and analyzed where fault-tolerant features have been implemented. In this configuration, an externally applied force larger than the design force does not damage the active components of the actuator. The actuator housing can be configured and produced using cost-effective methods such as injection molding, or alternatively, its components can be mounted directly on a small circuit board.

The actuator is driven by a SMA -NiTi as a primary active element, and it requires energy on the order of 20 Ws(J) per cycle. Electrical connections to points A and B are used to apply electrical power in the resistive NiTi wire, causing a phase change that contracts the wire on the order of 5%. The actuation period is of the order of a second for generating the stroke, and 4 to 10 seconds for resetting. Thus, this design allows the actuator to work at a frequency of up to 0.1 Hz.

The actuator does not make use of the whole range of motion of the SMA material, allowing for large margins on the mechanical parameters of the design. The efficiency of the actuator is of the order of 10%, including the margins. The average dissipated power while driving at full speed is of the order of 1 W, and can be scaled down linearly if the rate of cycling is reduced. This design produces an extremely quiet actuator; it can generate a force greater than 2 N and a stroke greater than 1 cm. The operational duration of SMA materials is of the order of millions of cycles with some reduced stroke over a wide temperature range up to 150 °C.

This work was done by Mircea Badescu, Stewart Sherrit, and Yoseph Bar-Cohen of Caltech for NASA's Jet Propulsion Laboratory. Further information is contained in a TSP (see page 1). ***NPO-47991***

Ultra-Compact Motor Controller

Applications include industrial robotic arms, industrial machinery, and automobiles.

Lyndon B. Johnson Space Center, Houston, Texas

This invention is an electronically commutated brushless motor controller that incorporates Hall-array sensing in a small, 42-gram package that provides 4096 absolute counts per motor revolution position sensing. The unit is the size of a miniature hockey puck, and is a 44-pin male connector that provides many I/O channels, including CANbus, RS-232 communications, general-purpose analog and digital I/O (GPIO), analog and digital Hall inputs, DC power input (18–90 VDC, 0–l0 A), three-phase motor outputs, and a strain gauge amplifier.

This controller replaces air cooling with conduction cooling via a high-thermal-conductivity epoxy casting. A secondary advantage of the relatively good heat conductivity that comes with ultra-small size is that temperature differences within the controller become smaller, so that it is easier to measure the hottest temperature in the controller with fewer temperature sensors, or even one temperature sensor.

Another size-sensitive design feature is in the approach to electrical noise immunity. At a very small size, where conduction paths are much shorter than in conventional designs, the ground becomes essentially isopotential, and so certain (space-consuming) electrical noise control components become unnecessary, which helps make small size possible. One winding-current sensor, applied to all of the windings in fast sequence, is smaller and wastes less power than the two or more sensors conventionally used to sense and control winding currents. An unexpected benefit of using only one current sensor is that it actually improves the precision of current control by using the "same" sensors to read each of the three phases. Folding the encoder directly into the controller electronics eliminates a great deal of redundant electronics, packaging, connectors, and hook-up wiring. The reduction of wires and connectors subtracts substantial bulk and eliminates their role in behaving as EMI (electromagnetic interference) antennas.

A shared knowledge by each motor controller of the state of all the motors in the system at 500 Hz also allows parallel processing of higher-level kinematic matrix calculations.

This work was done by William T. Townsend, Adam Crowell, and Traveler Hauptman of Barrett Technology, Inc.; and Gill Andrews Pratt of Olin College for Johnson Space Center. For further information, contact the JSC Innovation Partnerships Office at (281) 483-3809.

In accordance with Public Law 96-517, the contractor has elected to retain title to this invention. Inquiries concerning rights for its commercial use should be addressed to:

Barrett Technology, Inc.
625 Mount Auburn Street
Cambridge, MA 02138-4555
Phone No.: (617) 252-9000
Web site: www.barrett.com

Refer to MSC-23930-1, volume and number of this NASA Tech Briefs *issue, and the page number.*

Extreme Ionizing-Radiation-Resistant Bacterium

Deinococcus phoenicis sp. nov. can be used as an indicator for sterilization processes in food, aerospace, medical, and pharmaceutical applications.

NASA's Jet Propulsion Laboratory, Pasadena, California

There is a growing concern that desiccation and extreme radiation-resistant, non-spore-forming microorganisms associated with spacecraft surfaces can withstand space environmental conditions and subsequent proliferation on another solar body. Such forward contamination would jeopardize future life detection or sample return technologies. The prime focus of NASA's planetary protection efforts is the development of strategies for inactivating resistance-bearing microorganisms. Eradication techniques can be designed to target resistance-conferring microbial populations by first identifying and understanding their physiologic and biochemical capabilities that confers its elevated tolerance (as is being studied in *Deinococcus phoenicis*, as a result of this description). Furthermore, hospitals, food, and government agencies frequently use biological indicators to ensure the efficacy of a wide range of radiation-based sterilization processes. Due to their resistance to a variety of perturbations, the non-spore forming *D. phoenicis* may be a more appropriate biological indicator than those currently in use.

The high flux of cosmic rays during space travel and onto the unshielded surface of Mars poses a significant hazard to the survival of microbial life. Thus, radiation-resistant microorganisms are of particular concern that can survive extreme radiation, desiccation, and low temperatures experienced during space travel. Spore-forming bacteria, a common inhabitant of spacecraft assembly facilities, are known to tolerate these extreme conditions. Since the Viking era, spores have been utilized to assess the degree and level of microbiological contamination on spacecraft and their associated spacecraft assembly facilities. Members of the non-spore-forming bacterial community such as *Deinococcus radiodurans* can survive acute exposures to ionizing radiation (5 kGy), ultraviolet light (1 kJ/m^2), and desiccation (years). These resistive phenotypes of *Deinococcus* enhance the potential for transfer, and subsequent proliferation, on another solar body such as Mars and Europa. These organisms are more likely to escape planetary protection assays, which only take into account presence of spores. Hence, presences of extreme radiation-resistant *Deinococcus* in the cleanroom facility where spacecraft are assembled pose a serious risk for integrity of life-detection missions.

The microorganism described herein was isolated from the surfaces of the cleanroom facility in which the Phoenix Lander was assembled. The isolated bacterial strain was subjected to a comprehensive polyphasic analysis to characterize its taxonomic position. This bacterium exhibits very low 16SrRNA similarity with any other environmental isolate reported to date. Both phenotypic and phylogenetic analyses clearly indicate that this isolate belongs to the genus *Deinococcus* and represents a novel species. The name *Deinococcus phoenicis* was proposed after the Phoenix spacecraft, which was undergoing assembly, testing, and launch operations in the spacecraft assembly facility at the time of isolation. *D. phoenicis* cells exhibited higher resistance to ionizing radiation (cobalt-60; 14 kGy) than the cells of the *D. radiodurans* (5 kGy). Thus, it is in the best interest of NASA to thoroughly characterize this organism, which will further assess in determining the potential for forward contamination. Upon the completion of genetic and physiological characteristics of *D. phoenicis*, it will be added to a planetary protection database to be able to further model and predict the probability of forward contamination.

This work was done by Parag A. Vaishampayan and Kasthuri J. Venkateswaran of Caltech, and Petra Schwendner of Institute of Aerospace Medicine, German Aerospace Center (DLR), Germany for NASA's Jet Propulsion Laboratory. For more information, contact iaoffice@jpl.nasa.gov. NPO-48008

Wideband Single-Crystal Transducer for Bone Characterization

These transducers have uses in medical ultrasound imaging and room-temperature ultrasonic flow meters.

John H. Glenn Research Center, Cleveland, Ohio

The microgravity conditions of space travel result in unique physiological demands on the human body. In particular, the absence of the continual mechanical stresses on the skeletal system that are present on Earth cause the bones to decalcify. Trabecular structure decreases in thickness and increases in spacing, resulting in decreased bone strength and increased risk of injury. Thus, monitoring bone health is a high priority for long-term space travel. A single probe covering all frequency bands of interest would be ideal for such measurements, and this would also minimize storage space and eliminate the complexity of integrating multiple probes.

This invention is an ultrasound transducer for the structural characterization of bone. Such characterization meas-

ures features of reflected and transmitted ultrasound signals, and correlates these signals with bone structure metrics such as bone mineral density, trabecular spacing, and thickness, etc. The techniques used to determine these various metrics require measurements over a broad range of ultrasound frequencies, and therefore, complete characterization requires the use of several narrowband transducers.

This is a single transducer capable of making these measurements in all the required frequency bands. The device achieves this capability through a unique combination of a broadband piezoelectric material; a design incorporating multiple resonator sizes with distinct, overlapping frequency spectra; and a micromachining process for producing the multiple-resonator pattern with common electrode surfaces between the resonators.

This device consists of a pattern of resonator bars with common electrodes that is wrapped around a central mandrel such that the radiating faces of the resonators are coplanar and can be simultaneously applied to the sample to be measured. The device operates as both a source and receiver of acoustic energy. It is operated by connection to an electronic system capable of both providing an excitation signal to the transducer and amplifying the signal received from the transducer. The excitation signal may be either a wide-bandwidth signal to excite the transducer across its entire operational spectrum, or a narrow-bandwidth signal optimized for a particular measurement technique. The transducer face is applied to the skin covering the bone to be characterized, and may be operated in through-transmission mode using two transducers, or in pulse-echo mode.

The transducer is a unique combination of material, design, and fabrication technique. It is based on single-crystal lead magnesium niobate lead titanate (PMN-PT) piezoelectric material. As compared to the commonly used piezoceramics, this piezocrystal has superior piezoelectric and elastic properties, which results in devices with superior bandwidth, source level, and power requirements. This design necessitates a single resonant frequency. However, by operating in a transverse length-extensional mode, with the electric field applied orthogonally to the extensional direction, resonators of different sizes can share common electrodes, resulting in a multiply-resonant structure. With carefully sized resonators, and the superior bandwidth of piezocrystal, the resonances can be made to overlap to form a smooth, wide-bandwidth characteristic.

This work was done by Yu Liang and Kevin Snook of TRS Technologies, Inc. for Glenn Research Center. Further information is contained in a TSP (see page 1).

Inquiries concerning rights for the commercial use of this invention should be addressed to NASA Glenn Research Center, Innovative Partnerships Office, Attn: Steven Fedor, Mail Stop 4–8, 21000 Brookpark Road, Cleveland, Ohio 44135. Refer to LEW-18842-1.

Fluorescence-Activated Cell Sorting of Live Versus Dead Bacterial Cells and Spores

Commercial applications include hospital operating room cleanliness validation assays, pharmaceutical development, and semiconductor development.

NASA's Jet Propulsion Laboratory, Pasadena, California

This innovation is a coupled fluorescence-activated cell sorting (FACS) and fluorescent staining technology for purifying (removing cells from sampling matrices), separating (based on size, density, morphology, and live versus dead), and concentrating cells (spores, prokaryotic, eukaryotic) from an environmental sample.

Currently, the state of the art is limited to the sorting of larger eukaryotic cells (e.g., yeast, mammalian). Over the past decade, cell sorting technologies have evolved significantly and sensitivity levels have increased remarkably, rendering bacterial cell sorting a feasible concept. In parallel, optimized protocols for broad-spectrum fluorescence staining of bacterial cells and spores have been established, most of which are based on nucleic acid-intercalating dyes.

Smaller DNA-intercalating dyes, such as SYTO-9, permeate the intact membrane of living, viable cells and spores and upon excitation with white light, emit a detectable signal such as the green spectra emitted by DNA-bound SYTO-9. A larger DNA-intercalating dye such as 7- amino actinomycin (7-AAD), which is unable to permeate the membranes of healthy, viable cells and spores and thus only able to access the DNA of dead or dying cells and spores through compromised membranes, is also applied to the sample. This larger dye is engineered to fluoresce red spectra upon excitation. Ergo, the membranes of healthy, viable bacterial cells and spores preclude the infiltration of the larger red dyes (which have a greater affinity for DNA than the smaller green dyes) and as a result, their DNA fluoresces green. The DNA of dead or dying cells and spores fluoresces red as a result of the high-affinity binding and of the larger red dyes. This motif makes possible the ability to sort and segregate live from dead bacterial cells and spores via fluorescence staining.

This technology directly contributes to NASA missions as it focuses on the separation, purification, and concentration of cells or spores from a given spacecraft or associated facility sample. Coupling live/dead fluorescence dyes and flow cytometry enhances the resolving power of any attempt at predicting the microbial genetic that actually poses a forward contamination threat. The capability to provide an account of the living organisms present on spacecraft surfaces, to the exclusion of the expired population, will facilitate much more accurate predictive risk assessments of forward contamination on missions with challenging planetary protection issues. A specific account of only the living microbial population will also allow for immediate feedback to a project as to the success of cleaning, microbial reduction, and general housekeeping processes.

This work was done by James N. Benardini, Myron T. La Duc, Rochelle Diamond, and Josh Verceles of Caltech for NASA's Jet Propulsion Laboratory. Further information is contained in a TSP (see page 1). NPO-48176

Nonhazardous Urine Pretreatment Method

This method can be used as a means for safe urine storage on ships, planes, and recreational vehicles, or in conjunction with portable restrooms.

Lyndon B. Johnson Space Center, Houston, Texas

A method combines solid phase acidification with two non-toxic biocides to prevent ammonia volatilization and microbial proliferation. The safe, non-oxidizing biocide combination consists of a quaternary amine and a food preservative. This combination has exhibited excellent stabilization of both acidified and unacidified urine.

During pretreatment tests, composite urine collected from donors was challenged with a microorganism known to proliferate in urine, and then was processed using the nonhazardous urine pre-treatment method. The challenge microorganisms included *Escherichia coli*, a common gram-negative bacteria; *Enterococcus faecalis*, a ureolytic gram-positive bacteria; *Candida albicans*, a yeast commonly found in urine; and *Aspergillus niger*, a problematic mold that resists urine pre-treatment.

Urine processed in this manner remained microbially stable for over 57 days. Such effective urine stabilization was achieved using non-toxic, non-oxidizing biocides at higher pH (3.6 to 5.8) than previous methods in use or projected for use aboard the International Space Station (ISS). ISS urine pretreatment methods employ strong oxidants including ozone and hexavalent chromium (Cr(VI)), a carcinogenic material, under very acidic conditions (pH = 1.8 to 2.4).

The method described here offers a much more benign chemical environment than previous pretreatment methods, and will lower equivalent system mass (ESM) by reducing containment volume and mass, system complexity, and crew time needed to handle pre-treatment chemicals. The biocides, being non-oxidizing, minimize the potential for chemical reactions with urine constituents to produce volatile, airborne contaminants such as cyanogen chloride. Additionally, the biocides are active under significantly less acidic conditions than those used in the current system, thereby reducing the degree of required acidification.

A simple flow-through solid phase acidification (SPA) bed is employed to overcome the natural buffering capacity of urine, and to lower the pH to levels that fix ammoniacal nitrogen in the non-volatile and highly water soluble NH_4^+ form. Citric acid, a highly soluble, solid tricarboxylic acid essential to cellular metabolism, and typically used as a food preservative, has also been shown to efficiently acidify urine in conjunction with non-oxidizing biocides to provide effective stabilization with respect to both microbial growth and ammonia volatilization.

This work was done by James R. Akse and John T. Holtsnider of Umpqua Research Company for Johnson Space Center. For further information, contact the JSC Innovation Partnerships Office at (281) 483-3809. MSC-24520-1

Laser-Ranging Transponders for Science Investigations of the Moon and Mars

NASA's Jet Propulsion Laboratory, Pasadena, California

An active laser was developed ranging in real-time with two terminals, emulating interplanetary distances, and with submillimeter accuracy. In order to overcome the limitations to ranging accuracy from jitters and delay drifts within the transponders, architecture was proposed based on asynchronous paired one-way ranging with local references. A portion of the transmitted light is directed, via a reference path, to the local detector. This allows for compensation of any jitter in the timing of the emitted laser pulse. The same detector is used to measure the time of the received pulses emitted from the remote terminal. This approach removes any change in the delay caused by the detector or its electronics.

Two separate terminals using commercial off-the-shelf hardware were built to emulate active laser ranging over interplanetary distances. The communication link for the command to start recording pulse arrival times and data transfer from one terminal to the other was achieved using a standard wireless link, emulating free space laser communication. The deviation is well below the goal of 1-mm precision. This leaves enough margin to achieve 1-mm precision when including the fluctuations due to atmospheric turbulence while ranging to Mars through the Earth's atmosphere. The two terminals are mounted on translation stages, which can be moved freely on rails to yield a wide range of distances with fine adjustment. The two terminals were separated by approximately 16 meters.

This work was done by Hamid Hemmati, Yijiang Chen, and Kevin Birnbaum of Caltech for NASA's Jet Propulsion Laboratory. For more information, contact iaoffice@jpl.nasa.gov. NPO-48125

Ka-Band Waveguide Three-Way Serial Combiner for MMIC Amplifiers

This device is a power combiner that can be used for a solid-state power amplifier.

John H. Glenn Research Center, Cleveland, Ohio

In this innovation, the three-way combiner consists internally of two branch-line hybrids that are connected in series by a short length of waveguide. Each branch-line hybrid is designed to combine input signals that are in phase with an amplitude ratio of two. The combiner is constructed in an E-plane split-block arrangement and is precision machined from blocks of aluminum with standard WR-28 waveguide ports. The port impedances of the combiner are matched to that of a standard WR-28 waveguide. The component parts include the power combiner and the MMIC (monolithic microwave integrated circuit) power amplifiers (PAs). The three-way series power combiner is a six-port device. For basic operation, power that enters ports 3, 5, and 6 is combined in phase and appears at port 1. Ports 2 and 4 are isolated ports. The application of the three-way combiner for combining three PAs with unequal output powers was demonstrated.

NASA requires narrow-band solid-state power amplifiers (SSPAs) at Ka-band frequencies with output power in the range of 3 to 5 W for radio or gravity science experiments. In addition, NASA also requires wideband, high-efficiency SSPAs at Ka-band frequencies with output power in the range of 5 to 15 W for high-data-rate communications from deep space to Earth. The three-way power combiner is designed to operate over the frequency band of 31.8 to 32.3 GHz, which is NASA's deep-space frequency band.

For the proof-of-concept demonstration of this innovation, three available PAs were selected with output powers of 0.1, 0.2, and 0.6 W to meet the ampli-

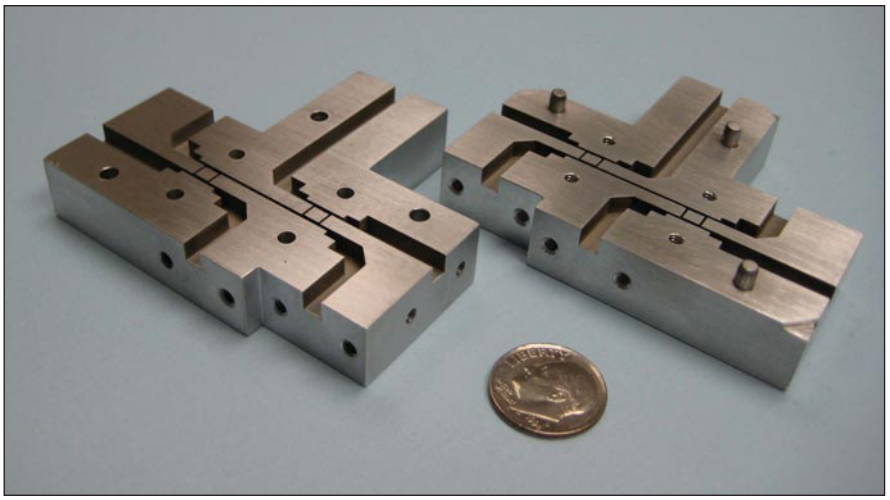

This photo of the fabricated **Serial Combiner** shows the split-block construction arrangement.

tude ratio of two. The 0.1- and 0.2-W PAs, which are in the 1:2 power ratio, are initially combined in a branch-line hybrid that has a coupling value of 4.77 dB. Likewise, the combined output of the first branch-line hybrid is combined with the output from the third PA in a second branch-line hybrid, also with a coupling value of 4.77 dB. The measured combining efficiency at the center frequency of 32.05 GHz is greater than 90% for a wide range of power ratios both below and above two. The measured return loss at the output port 1 and the isolation among the input ports 3, 5, and 6 of the three-way combiner are greater than 16 and 22 dB, respectively.

This work was done by Rainee N. Simons, Edwin G. Wintucky, and Jon C. Freeman of Glenn Research Center; and Christine T. Chevalier of QinetiQ North America Corp. Further information is contained in a TSP (see page 1).

Inquiries concerning rights for the commercial use of this invention should be addressed to NASA Glenn Research Center, Innovative Partnerships Office, Attn: Steven Fedor, Mail Stop 4–8, 21000 Brookpark Road, Cleveland, Ohio 44135. Refer to LEW-18688-1

Structural Health Monitoring With Fiber Bragg Grating and Piezo Arrays

A nondestructive damage identification and assessment capability can be used in monitoring systems for maintenance and disaster avoidance.

Dryden Flight Research Center, Edwards, California

Structural health monitoring (SHM) is one of the most important tools available for the maintenance, safety, and integrity of aerospace structural systems. Lightweight, electromagnetic-interference-immune, fiber-optic sensor-based SHM will play an increasing role in more secure air transportation systems. Manufacturers and maintenance personnel have pressing needs for significantly improving safety and reliability while providing for lower inspection and maintenance costs. Undetected or untreated damage may grow and lead to catastrophic structural failure.

Damage can originate from the strain/stress history of the material, imperfections of domain boundaries in metals, delamination in multi-layer materials, or the impact of machine tools in the manufacturing process. Damage can likewise develop during service life from wear and tear, or under extraordinary circumstances such as with unusual forces, temperature cycling, or impact of flying objects. Monitoring and early detection are key to preventing a catastrophic failure of structures, especially when these are expected to perform near their limit conditions.

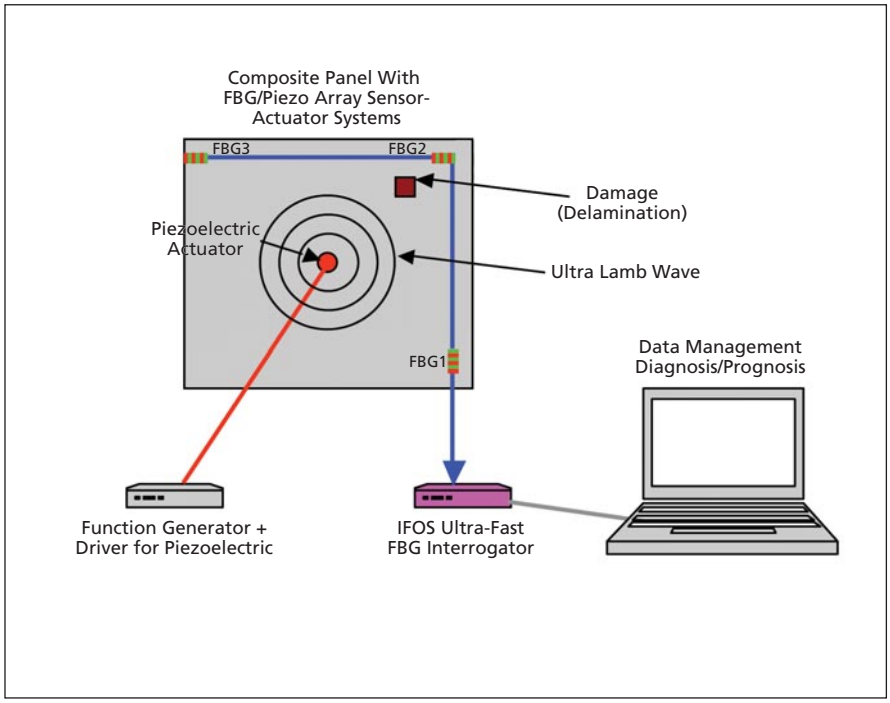

The **Fiber Bragg Grating/Piezo Array** sensor-actuator system as a concept demonstration for structural health monitoring.

The ultimate goal of SHM technology is to develop autonomous (preventive) maintenance systems for continuous monitoring, inspection, and damage detection of structures with minimum labor involvement in real time, and in order to prevent catastrophic structural failure with timely service/maintenance. The ultimate solution will include both advanced hardware and advanced mathematical algorithms.

On the hardware side, a high-speed, high-channel-count fiber-optic sensor interrogation system was developed. On the SHM algorithmic side, algorithmic methods were developed for characterizing the damage from sensory data collected over several strategically placed sensors.

A dynamic response-based damage detection technique is relatively easy to implement and offers a wealth of differential diagnostic capabilities. The basic assumptions of this technique are that the dynamic parameters such as natural frequencies, mode shapes, transfer functions, or response functions depend on the physical properties across the structures. Therefore, the changes in these dynamic characteristics can be used to locate and assess problem areas. Smart optical fiber Bragg grating (FBG) sensors have been increasingly used in SHM, and they could be either surface-bonded or embedded within the structures, and form an array of sensors for dynamic response measurement. For a small-scale demonstration, Lamb waves are excited by a single piezoelectric actuator and captured by three FBG sensors whose response is in turn captured by a parallel processing FBG interrogator ca-

pable of sampling each sensor simultaneously at hundreds of kilohertz. The number of sensors required for damage detection is fewer than low-frequency techniques that can also use FBGs, such as those based on the mode shapes of the structure.

This work was done by Richard J. Black, Ferey Faridian, Behzad Moslehi, and Vahid Sotoudeh of Intelligent Fiber Optic Systems Corporation (IFOS) for Dryden Flight Research Center. Further information is contained in a TSP (see page 1). DRC-010-015

Low-Gain Circularly Polarized Antenna With Torus-Shaped Pattern

A shaped aperture is used, and rather than the standard linear bicone, a parabolic bicone was found to reduce the amount of phase variation as the aperture increases.

NASA's Jet Propulsion Laboratory, Pasadena, California

The Juno mission to Jupiter requires an antenna with a torus-shaped antenna pattern with approximately 6 dBic gain and circular polarization over the Deep Space Network (DSN) 7-GHz transmit frequency and the 8-GHz receive frequency. Given the large distances that accumulate en-route to Jupiter and the limited power afforded by the solar-powered vehicle, this toroidal low-gain antenna requires as much gain as possible while maintaining a beam width that could facilitate a ±10° edge of coverage.

The natural antenna that produces a toroidal antenna pattern is the dipole, but the limited ≈2.2 dB peak gain would be insufficient. Here a shaped variation of the standard bicone antenna is proposed that could achieve the required gains and bandwidths while maintaining a size that was not excessive. The final geometry that was settled on consisted of a corrugated, shaped bicone, which is fed by a WR112 waveguide-to-coaxial-waveguide transition. This toroidal low-gain antenna (TLGA) geometry produced the requisite gain, moderate sidelobes, and the torus-shaped antenna pattern while maintaining a very good match over the entire required frequency range. Its "horn" geometry is also low-loss and capable of handling higher powers with large margins against multipactor breakdown. The final requirement for the antenna was to link with the DSN with circular polarization. A four-layer meander-line array polarizer was implemented; an approach that was fairly well suited to the TLGA geometry.

The principal development of this work was to adapt the standard linear bicone such that its aperture could be increased in order to increase the available gain of the antenna. As one increases the aperture of a standard bicone, the phase variation across the aperture begins to increase, so the larger the aperture becomes, the greater the phase variation. In order to maximize the gain from any aperture antenna, the phase should be kept as uniform as possible. Thus, as the standard bicone's aperture increases, the gain increase becomes less until one reaches a point of diminishing returns.

In order to overcome this problem, a shaped aperture is used. Rather than the standard linear bicone, a parabolic bicone was found to reduce the amount of phase variation as the aperture increases. In fact, the phase variation is half of the standard linear bicone, which leads to higher gain with smaller aperture sizes. The antenna pattern radiated from this parabolic-shaped bicone antenna has fairly high side lobes. The Juno project requested that these sidelobes be minimized. This was accomplished by adding corrugations to the parabolic shape. This corrugated-shaped bicone antenna had reasonably low sidelobes, and the appropriate gain and beamwidth to meet project requirements.

This work was done by Luis R. Amaro, Ronald C. Kruid, and Joseph D. Vacchione of Caltech, and Aluizio Prata of University of Southern California for NASA's Jet Propulsion Laboratory. For more information, contact iaoffice@jpl.nasa.gov. NPO-48320

Software

Stereo and IMU-Assisted Visual Odometry for Small Robots

This software performs two functions: (1) taking stereo image pairs as input, it computes stereo disparity maps from them by cross-correlation to achieve 3D (three-dimensional) perception; (2) taking a sequence of stereo image pairs as input, it tracks features in the image sequence to estimate the motion of the cameras between successive image pairs. A real-time stereo vision system with IMU (inertial measurement unit)-assisted visual odometry was implemented on a single 750 MHz/520 MHz OMAP3530 SoC (system on chip) from TI (Texas Instruments). Frame rates of 46 fps (frames per second) were achieved at QVGA (Quarter Video Graphics Array i.e. 320×240), or 8 fps at VGA (Video Graphics Array 640×480) resolutions, while simultaneously tracking up to 200 features, taking full advantage of the OMAP3530's integer DSP (digital signal processor) and floating point ARM processors. This is a substantial advancement over previous work as the stereo implementation produces 146 Mde/s (millions of disparities evaluated per second) in 2.5W, yielding a stereo energy efficiency of 58.8 Mde/J, which is 3.75× better than prior DSP stereo while providing more functionality.

The focus is on stereo vision and IMU-aided visual odometry for small unmanned ground vehicle applications. It is expected that elements of this implementation will carry over to small unmanned air vehicles in future work. Because the objective is to advance the state of the art in compact, low-power implementation for small robots, highly efficient algorithms that have already been field tested have been chosen. This system combines the sum of absolute differences (SAD)-based, local optimization stereo with two-frame visual odometry using FAST features (Features from Accelerated Segment Test). By exploiting the dense depth map to provide stereo correspondence for the FAST features, it achieves very respectable position errors of 0.35% of distance traveled on datasets covering 400 m of travel. The algorithms used by this system were heavily tested in previous projects, which gives a solid basis for their implementation on the OMAP3530. In the future, cost/performance trade-offs of algorithm variants may be explored.

The novelty of this system is the parallel computation of stereo vision and visual odometry on both cores of the OMAP SoC. All stereo-related computation is handled on the C64x+ side of the OMAP, while feature detection, matching/tracking, and egomotion estimation is handled on the ARM side. This is a convenient division of processing, as stereo computation is entirely an integer process, well suited to the integer only C64x+, while several parts of visual odometry involve floating point operations. The TI codec engine's IUniversal wrapper was used to integrate the ARM and DSP processes.

This work was done by Larry H. Matthies of Caltech and Steven B. Goldberg of Indelible Systems Inc. for NASA's Jet Propulsion Laboratory. ***For more information, download the Technical Support Package (free white paper) at www.techbriefs.com/tsp under the Software category****.*

The software used in this innovation is available for commercial licensing. Please contact Daniel Broderick of the California Institute of Technology at danielb@caltech.edu. Refer to NPO-48103.

Global Swath and Gridded Data Tiling

This software generates cylindrically projected tiles of swath-based or gridded satellite data for the purpose of dynamically generating high-resolution global images covering various time periods, scaling ranges, and colors called "tiles." It reconstructs a global image given a set of tiles covering a particular time range, scaling values, and a color table. The program is configurable in terms of tile size, spatial resolution, format of input data, location of input data (local or distributed), number of processes run in parallel, and data conditioning.

This software can dynamically generate global images of various temporal and spatial resolutions without having to go back to the original data files, reading and conditioning, and re-projecting the source values. It can be utilized to efficiently generate global imagery of various temporal and spatial resolutions based upon cylindrically projected tiles that have been created from swath and gridded data sets.

The package supports JPL's Physical Oceanography Distributed Active Archive Center's (PO.DAAC) State of the Ocean Web page (http://podaac.jpl.nasa.gov/soto), a Google Earth-based Web interactive visualization tool.

This work was done by Charles K. Thompson of Caltech for NASA's Jet Propulsion Laboratory. For more information, contact iaoffice@jpl.nasa.gov.

This software is available for commercial licensing. Please contact Daniel Broderick of the California Institute of Technology at danielb@caltech.edu. Refer to NPO-48113.

GOES-R: Satellite Insight

GOES-R: Satellite Insight seeks to bring awareness of the GOES-R (Geostationary Operational Environmental Satellite — R Series) satellite currently in development to an audience of all ages on the emerging medium of mobile games. The iPhone app (Satellite Insight) was created for the GOES-R Program. The app describes in simple terms the types of data products that can be produced from GOES-R measurements. The game is easy to learn, yet challenging for all audiences. It includes educational content and a path to further information about GOES-R, its technology, and the benefits of the data it collects.

The game features action-puzzle game play in which the player must prevent an overflow of data by matching falling blocks that represent different types of GOES-R data. The game adds more different types of data blocks over time, as long as the player can prevent a data overflow condition. Points are awarded for matches, and players can compete with themselves to beat their highest score.

This work was done by Austin J. Fitzpatrick, Nancy J. Leon, Alexander Novati, Laura K. Lincoln, and Diane K. Fisher of Caltech, and Daniel Karlson of NOAA for NASA's Jet Propulsion Laboratory. For more information, contact iaoffice@jpl.nasa.gov.

This software is available for commercial licensing. Please contact Daniel Broderick of the California Institute of Technology at danielb@caltech.edu. Refer to NPO-48264.

Aquarius iPhone Application

The Office of the CIO at JPL has developed an iPhone application for the Aquarius/SAC-D mission. The application includes specific information about

the science and purpose of the Aquarius satellite and also features daily mission news updates pulled from sources at Goddard Space Flight Center as well as Twitter. The application includes a media and data tab section. The media section displays images from the observatory, viewing construction up to the launch and also includes various videos and recorded diaries from the Aquarius Project Manager. The data tab highlights many of the factors that affect the Earth's ocean and the water cycle. The application leverages the iPhone's accelerometer to move the Aquarius Satellite over the Earth, revealing these factors. Lastly, this application features a countdown timer to the satellite's launch, which is currently counting the days since launch. This application was highly successful in promoting the Aquarius Mission and educating the public about how ocean salinity is paramount to understanding the Earth.

This is a public application available at the time of this reporting in The Apple App Store: http://itunes.apple.com/us/app/aquarius/id437313730?mt=8

This work was done by Joseph C. Estes Jr, Jeremy M. Arca, Michael A. Ko, and Boris Oks of Caltech for NASA's Jet Propulsion Laboratory. For more information, contact iaoffice@jpl.nasa.gov.

This software is available for commercial licensing. Please contact Daniel Broderick of the California Institute of Technology at danielb@caltech.edu. Refer to NPO-48177.

Monitoring of International Space Station Telemetry Using Shewhart Control Charts

This technique can be applied to monitoring critical systems such as electrical power generation and manufacturing equipment.

Lyndon B. Johnson Space Center, Houston, Texas

Shewhart control charts have been established as an expedient method for analyzing dynamic, trending data in order to identify anomalous subsystem performance as soon as such performance would exceed a statistically established baseline. Additionally, this leading indicator tool integrates a selection methodology that reduces false positive indications, optimizes true leading indicator events, minimizes computer processor unit duty cycles, and addresses human factor concerns (i.e., the potential for flight-controller data overload). This innovation leverages statistical process control, and provides a relatively simple way to allow flight controllers to focus their attention on subtle system changes that could lead to dramatic off-nominal system performance. Finally, this capability improves response time to potential hardware damage and/or crew injury, thereby improving space flight safety.

Shewhart control charts require normalized data. However, the telemetry from the ISS Early External Thermal Control System (EETCS) was not normally distributed. A method for normalizing the data was implemented, as was a means of selecting data windows, the number of standard deviations (Sigma Level), the number of consecutive points out of limits (Sequence), and direction (increasing or decreasing trend data). By varying these options, and treating them like dial settings, the number of nuisance alerts and leading indicators were optimized. The goal was to capture all leading indicators while minimizing the number of nuisances. Lean Six Sigma (L6S) design of experiment methodologies were employed. To optimize the results, Perl programming language was used to automate the massive amounts of telemetry data, control chart plots, and the data analysis.

This work was done by Jeffery T. Fitch, Alan L. Simon, John A. Gouveia, Andrew M. Hillin, and Steve A. Hernandez of United Space Alliance for Johnson Space Center. Further information is contained in a TSP (see page 1). ***MSC-24530-1***

Theory of a Traveling Wave Feed for a Planar Slot Array Antenna

A design procedure was developed for the coupling slots between the feed waveguide and the radiating waveguides.

NASA's Jet Propulsion Laboratory, Pasadena, California

Planar arrays of waveguide-fed slots have been employed in many radar and remote sensing applications. Such arrays are designed in the standing wave configuration because of high efficiency. Traveling wave arrays can produce greater bandwidth at the expense of efficiency due to power loss in the load or loads. Traveling wave planar slot arrays may be designed with a long feed waveguide consisting of centered-inclined coupling slots. The feed waveguide is terminated in a matched load, and the element spacing in the feed waveguide is chosen to produce a beam squinted from the broadside.

The traveling wave planar slot array consists of a long feed waveguide containing resonant-centered inclined coupling slots in the broad wall, coupling power into an array of stacked radiating waveguides orthogonal to it. The radiating waveguides consist of longitudinal offset radiating slots in a standing wave configuration. For the traveling wave feed of a planar slot array, one has to design the tilt angle and length of each coupling slot such that the amplitude and phase of excitation of each radiating waveguide are close to the desired values. The coupling slot spacing is chosen for an appropriate beam squint. Scattering matrix parameters of resonant coupling slots are used in the design process to produce appropriate excitations of radiating waveguides with constraints placed only on amplitudes.

Since the radiating slots in each radiating waveguide are designed to produce a certain total admittance, the scattering (S) matrix of each coupling slot is reduced to a 2×2 matrix. Elements of each 2×2 S-matrix and the amount of coupling into the corresponding radiating waveguide are expressed in terms of the element S_{11}. S matrices are converted into transmission (T) matrices, and the T matrices are multiplied to cascade the coupling slots and waveguide sections, starting from the load end and proceeding towards the source.

While the use of non-resonant coupling slots may provide an additional degree of freedom in the design, resonant coupling slots simplify the design process. The amplitude of the wave going to the load is set at unity. The S_{11} parameter, r' of the coupling slot closest to the load, is assigned an arbitrary

value. A larger value of r' will reduce the power dissipated in the load while increasing the reflection coefficient at the input port. It is now possible to obtain the excitation of the radiating waveguide closest to the load and the coefficients of the wave incident and reflected at the input port of this coupling slot. The next coupling slot parameter, r', is chosen to realize the excitation of that radiating waveguide. One continues this process moving towards the source, until all the coupling slot parameters r' and hence the S_{11} parameter of the 4-port coupler, r, are known for each coupling slot. The goal is to produce the desired array aperture distribution in the feed direction. From an interpolation of the computed moment method data for the slot parameters, all the coupling slot tilt angles and lengths are obtained. From the excitations of the radiating waveguides computed from the coupling values, radiating slot parameters may be obtained so as to attain the desired total normalized slot admittances. This process yields the radiating slot parameters, offsets, and lengths. The design is repeated by choosing different values of r' for the last coupling slot until the percentage of power dissipated in the load and the input reflection coefficient values are satisfactory.

Numerical results computed for the radiation pattern, the tilt angles and lengths of coupling slots, and excitation phases of the radiating waveguides, are presented for an array with uniform amplitude excitation. The design process has been validated using computer simulations. This design procedure is valid for non-uniform amplitude excitations as well.

This work was done by Sembiam Rengarajan of Caltech for NASA's Jet Propulsion Laboratory. For more information, contact iaoffice@jpl.nasa.gov. NPO-48221

Time Manager Software for a Flight Processor

John F. Kennedy Space Center, Florida

Data analysis is a process of inspecting, cleaning, transforming, and modeling data to highlight useful information and suggest conclusions. Accurate timestamps and a timeline of vehicle events are needed to analyze flight data. When data is gathered onboard a rocket, precise time stamping is even more important due to the rocket's high speeds and the requirement to integrate data over time for inertial navigation calculations.

Accurately time-tagging data currently requires an additional accurate timecode generator board. This solution is costly but is usually adequate for ground-based systems. However, this solution is not adequate for flight processors on rockets. Rocket systems require more costly ruggedized equipment where weight, size, and power constraints are an issue. Redundancy is also required, adding even more to the system's weight, size, and power consumption.

By moving the timekeeping to the flight processor, there is no longer a need for a redundant time source. If each flight processor is initially synchronized to GPS, they can freewheel and maintain a fairly accurate time throughout the flight with no additional GPS time messages received. However, additional GPS time messages will ensure an even greater accuracy.

Some modern microprocessors maintain a 64-bit internal time-base register that is incremented by a crystal oscillator, usually with a 20- to 100-MHz frequency. This time-base register can be read in an interrupt service routine (ISR) generated by the 1 pps signal from the GPS receiver. Next, a GPS time message is received. The time-base count is associated with the GPS time message time.

When a timestamp is required, a get-time function is called that immediately reads the time-base register. A delta count is calculated from the last GPS sync. The current time is calculated by adding this delta time to the last sync time. This process calculates a timestamp with an accuracy measured in microseconds, depending on the processor clock speed and the accuracy of the processor clock. If a 1 pps GPS ISR is not available, the time base register can be synchronized with the receipt of the GPS time message. If the microprocessor does not have a 64-bit internal time-base register, a count-down timer can be used.

This work was done by Roger Zoerner of ASRC Aerospace Corporation for Kennedy Space Center. For more information, contact the Kennedy Space Center Innovative Partnerships Office at 321-867-5033. KSC-13406

Simulation of Oxygen Disintegration and Mixing With Hydrogen or Helium at Supercritical Pressure

These models can be used in simulations of gas turbine engines.

NASA's Jet Propulsion Laboratory, Pasadena, California

The simulation of high-pressure turbulent flows, where the pressure, p, is larger than the critical value, p_c, for the species under consideration, is relevant to a wide array of propulsion systems, e.g. gas turbine, diesel, and liquid rocket engines. Most turbulence models, however, have been developed for atmospheric-p turbulent flows. The difference between atmospheric-p and supercritical-p turbulence is that, in the former situation, the coupling between dynamics and thermodynamics is moderate to negligible, but for the latter it is very significant, and can dominate the flow characteristics. The reason for this stems from the mathematical form of the equation of state (EOS), which is the

perfect-gas EOS in the former case, and the real-gas EOS in the latter case.

For flows at supercritical pressure, p, the large eddy simulation (LES) equations consist of the differential conservation equations coupled with a real-gas EOS. The equations use transport properties that depend on the thermodynamic variables. Compared to previous LES models, the differential equations contain not only the subgrid scale (SGS) fluxes, but also new SGS terms, each denoted as a "correction." These additional terms, typically assumed null for atmospheric pressure flows, stem from filtering the differential governing equations, and represent differences between a filtered term and the same term computed as a function of the filtered flow field. In particular, the energy equation contains a heat-flux correction (q-correction) that is the difference between the filtered divergence of the heat flux and the divergence of the heat flux computed as a function of the filtered flow field. In a previous study, there was only partial success in modeling the q-correction term, but in this innovation, success has been achieved by using a different modeling approach.

This analysis, based on a temporal mixing layer Direct Numerical Simulation database, shows that the focus in modeling the q-correction should be on reconstructing the primitive variable gradients rather than their coefficients, and proposes the approximate deconvolution model (ADM) as an effective means of flow field reconstruction for LES heat flux calculation. Further, results for a study conducted for temporal mixing layers initially containing oxygen in the lower stream, and hydrogen or helium in the upper stream, show that, for any LES, including SGS-flux models (constant-coefficient Gradient or Scale-Similarity models, dynamic-coefficient Smagorinsky/Yoshizawa or mixed Smagorinsky/Yoshizawa/Gradient models), the inclusion of the q-correction in the LES leads to the theoretical maximum reduction of the SGS heat-flux difference. The remaining error in modeling this new subgrid term is thus irreducible.

This work was done by Josette Bellan and Ezgi Taskinoglu of Caltech for NASA's Jet Propulsion Laboratory. For more information, contact iaoffice@jpl.nasa.gov. NPO-47645

Books & Reports

A Superfluid Pulse Tube Refrigerator Without Moving Parts for Sub-Kelvin Cooling

A report describes a pulse tube refrigerator that uses a mixture of ^{3}He and superfluid ^{4}He to cool to temperatures below 300 mK, while rejecting heat at temperatures up to 1.7 K. The refrigerator is driven by a novel thermodynamically reversible pump that is capable of pumping the ^{3}He–^{4}He mixture without the need for moving parts.

The refrigerator consists of a reversible thermal magnetic pump module, two warm heat exchangers, a recuperative heat exchanger, two cold heat exchangers, two pulse tubes, and an orifice. It is two superfluid pulse tubes that run 180° out of phase. All components of this machine except the reversible thermal pump have been demonstrated at least as proof-of-concept physical models in previous superfluid Stirling cycle machines. The pump consists of two canisters packed with pieces of gadolinium gallium garnet (GGG). The canisters are connected by a superleak (a porous piece of VYCOR® glass). A superconducting magnetic coil surrounds each of the canisters.

This work was done by Franklin K. Miller of for Goddard Space Flight Center. Further information is contained in a TSP (see page 1). *GSC-15580-1*

Sapphire Viewports for a Venus Probe

A document discusses the creation of a viewport suitable for use on the surface of Venus. These viewports are rated for 500 °C and 100 atm pressure with appropriate safety factors and reliability required for incorporation into a Venus Lander. Sapphire windows should easily withstand the chemical, pressure, and temperatures of the Venus surface. Novel fixture designs and seals appropriate to the environment are incorporated, as are materials compatible with exploration vessels. A test cell was fabricated, tested, and leak rate measured. The window features polish specification of the sides and corners, soft metal padding of the sapphire, and a metal C-ring seal. The system safety factor is greater than 2, and standard mechanical design theory was used to size the window, flange, and attachment bolts using available material property data. Maintenance involves simple cleaning of the window aperture surfaces. The only weakness of the system is its moderate rather than low leak rate for vacuum applications.

This work was done by Stephen Bates of Thoughtventions Unlimited for Goddard Space Flight Center. Further information is contained in a TSP (see page 1). *GSC-16095-1*

The Mobile Chamber

A document discusses a simulation chamber that represents a shift from the thermal-vacuum chamber stereotype. This innovation, currently in development, combines the capabilities of space simulation chambers, the user-friendliness of modern-day electronics, and the modularity of plug-and-play computing. The Mobile Chamber is a customized test chamber that can be deployed with great ease, and is capable of bringing payloads at temperatures down to 20 K, in high vacuum, and with the desired metrology instruments integrated to the systems control. Flexure plans to lease Mobile Chambers, making them affordable for smaller budgets and available to a larger customer base.

A key feature of this design will be an Apple iPad-like user interface that allows someone with minimal training to control the environment inside the chamber, and to simulate the required extreme environments. The feedback of thermal, pressure, and other measurements is delivered in a 3D CAD model of the chamber's payload and support hardware. This GUI will provide the user with a better understanding of the payload than any existing thermal-vacuum system.

This work was done by Gregory Scharfstein and Russell Cox of Flexure LLC for Goddard Space Flight Center. Further information is contained in a TSP (see page 1). *GSC-16469-1*

Electric Propulsion Induced Secondary Mass Spectroscopy

A document highlights a means to complement remote spectroscopy while also providing *in situ* surface samples without a landed system. Historically, most compositional analysis of small body surfaces has been done remotely by analyzing reflection or nuclear spectra. However, neither provides direct measurement that can unambiguously constrain the global surface composition and most importantly, the nature of trace composition and second-phase impurities.

Recently, missions such as Deep Space 1 and Dawn have utilized electric propulsion (EP) accelerated, high-energy collimated beam of Xe^+ ions to propel deep space missions to their target bodies. The energies of the Xe^+ are sufficient to cause sputtering interactions, which eject material from the top microns of a targeted surface. Using a mass spectrometer, the sputtered material can be determined. The sputtering properties of EP exhaust can be used to determine detailed surface composition of atmosphereless bodies by electric propulsion induced secondary mass spectroscopy (EPI-SMS).

EPI-SMS operation has three high-level requirements: EP system, mass spectrometer, and altitude of about 10 km. Approximately 1 keV Xe^+ has been studied and proven to generate high sputtering yields in metallic substrates. Using these yields, first-order calculations predict that EPI-SMS will yield high signal-to-noise at altitudes greater than 10 km with both electrostatic and Hall thrusters.

This work was done by Rashied Amini of Caltech and Geoffrey Landis of Glenn Research Center for NASA's Jet Propulsion Laboratory. Further information is contained in a TSP (see page 1). *NPO-47798*

Radiation-Tolerant DC-DC Converters

A document discusses power converters suitable for space use that meet the DSCC MIL-PRF-38534 Appendix G radiation hardness level P classification. A method for qualifying commercially produced electronic parts for DC-DC converters per the Defense Supply Center Columbus (DSCC) radiation hardened assurance requirements was developed.

Development and compliance testing of standard hybrid converters suitable for space use were completed for missions with total dose radiation requirements of up to 30 kRad. This innovation provides the same overall

performance as standard hybrid converters, but includes assurance of radiation-tolerant design through components and design compliance testing. This availability of design-certified radiation-tolerant converters can significantly reduce total cost and delivery time for power converters for space applications that fit the appropriate DSCC classification (30 kRad).

This work was done by Glenn Skutt, Dan Sable, Leonard Leslie, and Shawn Graham of VPT, Inc. for Johnson Space Center. Further information is contained in a TSP (see page 1). MSC-24497-1


NASA
National Aeronautics and
Space Administration